

The ghost-gluon vertex
in Landau gauge Yang-Mills theory
in four and three dimensions

WOLFGANG SCHLEIFENBAUM

Diplomarbeit
TU Darmstadt
Dezember 2004

Contents

1	Introduction	4
2	Green functions of Yang-Mills theory	5
2.1	Generating functional formalism	5
2.2	Yang-Mills theories	7
2.3	Landau gauge	11
3	Dyson-Schwinger equations	12
3.1	Derivation of Dyson-Schwinger equations	12
3.2	Truncation	14
3.3	Dyson-Schwinger equations for the ghost- and gluon propagator	14
3.4	Dyson-Schwinger equation for the ghost-gluon vertex	15
4	Propagators of Yang-Mills theory	16
4.1	Vertex approximations	16
4.2	Previous results	17
4.3	Implications for gluon confinement	18
5	Analytical structure of the ghost-gluon vertex	19
5.1	Lorentz structure	19
5.2	Symmetry	20
5.3	Slavnov-Taylor identity	21
6	Results	22
6.1	Perturbative results	23
6.2	Non-perturbative results	28
7	Conclusions	38
A	Notations	41
A.1	Conventions	41
A.2	Structure constants	41

B Derivation of the DSE for the ghost-gluon vertex	42
C Integrals	46
C.1 Vector integrals	46
C.2 Tensor integrals	47
C.3 Two-point integral	47
C.4 Triangle integral	48
D Integral kernels	49
E Infrared limits	50

1 Introduction

The physics of strong interaction is firmly believed to be governed by the theory of *Quantum Chromodynamics* (QCD) [Mut98]. Its degrees of freedom, the quarks and gluons, build the matter and the interactions the hadronic world consists of. The hadrons which are observed in experiments are colorless particle states in which the quarks and gluons are confined. The problem of explaining the confinement phenomenon has been long-standing. Also, dynamical chiral symmetry breaking which should explain the mass of hadrons, is a mechanism that is not yet completely understood.

Quantum field theories such as *Quantum Electrodynamics* (QED) have been developed and elaborated on in the last century especially by means of perturbation theory. For QED, this approach successfully describes the observations from low-energy experiments. QCD, on the other hand, is accessible by perturbation theory only for high energies where the theory is asymptotically free [Gro73, Pol73]. The phenomenon of confinement is, however, present for long range correlations, i.e. at low energy, where the strength of the coupling demands a non-perturbative treatment.

Non-perturbative methods in QCD are in general cumbersome. The complexity of the mathematical structure requires either immense computational power, as in lattice theory, or controlled approximations. One simplifying step is to neglect the influence of quarks and to consider *Yang-Mills* (YM) *theories* [Yan54] instead. For the high-temperature phase of QCD, the neglect of fermions is justified since the four-dimensional theory reduces to a three-dimensional Euclidian theory and a sum over Matsubara frequencies of which in the infinite temperature limit only the first bosonic mode has to be taken into consideration [App81, Das97]. For small temperatures, the neglect of fermions is expected to cause only a small effect on the dynamics of the gauge sector [Fis03]. For the investigation of the whole range of QCD's phase diagram at zero chemical potential, calculations in both four and three dimensions are therefore of physical interest.

A non-perturbative approach on solving a quantum field theory is the Dyson-Schwinger formalism [Dys49, Sch51]. It provides a set of integral equations which are the quantum equations of motion of the Green functions of the theory. If the *Dyson-Schwinger equations* (DSEs) were solved successfully, the whole variety of dynamics would be unveiled. The obstacle to be overcome with these integral equations is their mutual nonlinear coupling. Only by means of a truncation which decouples a subset of the DSEs it is possible to arrive at approximate solutions for the Green functions. Controlling the truncation induced errors is an important and difficult task. The ghost-gluon vertex, in particular, is a Green function that has some well-known properties in the Landau gauge and thus provides guidance for choosing a truncation. In recent Landau gauge studies [Sme98b, Alk01, Fis02, Maa04], the assumption was made that the ghost-gluon vertex could be substituted by its tree-level form. By doing so, a solution of a truncated set of DSEs was made possible and it yields the desired physical features including scenarios of confinement for the YM sector. The validity of these results depend, however, very sensitively on the legitimation of the assumption

concerning the ghost-gluon vertex. Hence, an investigation of this issue is imperative.

The intent of this work is to try and assess the assumption that the ghost-gluon vertex can be chosen in its tree-level form for Landau gauge Yang-Mills studies. This is, of course, of formal theoretical interest. Furthermore, it provides a check on the validity of recent DSE calculations and thus a better insight into the confinement mechanism of QCD.

This thesis is organized as follows. In section 2 the framework for Yang-Mills theories will be introduced. Provided with the formalism, the DSEs for the propagators and the ghost-gluon vertex can be investigated in section 3. In this context, the issue of truncation will be discussed. The results for the propagators which have been obtained in recent DSE studies under certain approximations will be presented in section 4 and later employed for the study of the ghost-gluon vertex. In section 5 the analytical structure of the vertex will be examined and in section 6 the results which have been found analytically and numerically will be shown and discussed. Finally, a conclusion will be given.

2 Green functions of Yang-Mills theory

The n -point Green functions of a quantum field theory are the vacuum expectation values of its n -point correlation functions. If we know how the fields are correlated in the vacuum then we know everything about the theory. A formalism that provides access to the Green functions is therefore desirable. In this section the path integral method will be employed to introduce generating functionals of various classifications of Green functions of a general quantum field theory. To become more specific, then the Green functions of YM theory that play the main roles for this work will be introduced. Some of the characteristics of the theory will be outlined.

2.1 Generating functional formalism

By virtue of the path integral method, an introduction can be found for in [Riv87], the formalism of functionals which generate the Green functions of a quantum field theory is briefly described. Consider a theory of a general set φ of fields, comprising bosonic fields φ_B^i and fermionic fields $\varphi_F^i, \bar{\varphi}_F^i$. The indices represent field, spacetime dependence as well as all other possible indices. Let the theory be governed by an action $\mathcal{S}[\varphi]$ given as a functional of these fields. Then from the partition sum

$$Z[\eta] = \int \mathcal{D}\varphi \exp \left(-\mathcal{S}[\varphi] + \varphi_B^i \eta_B^i + \bar{\varphi}_F^i \eta_F^i + \bar{\eta}_F^i \varphi_F^i \right), \quad (1)$$

all physical observables can be derived. Z depends on the set η incorporating external sources η_B^i for the bosonic fields as well as Grassmannian sources η_F^i and $\bar{\eta}_F^i$ for the fermionic fields $\bar{\varphi}_F^i$ and φ_F^i , respectively. The Einstein sum convention here generalizes to integration

2 GREEN FUNCTIONS OF YANG-MILLS THEORY

over d -dimensional spacetime such that it is understood that $\varphi_B^i \eta_B^i = \int d^d x \varphi_B^a(x) \eta_B^a(x)$, and equivalently for fermionic fields. It is assumed that the measure $\mathcal{D}\varphi$ is well-defined.

In the following sense the partition sum is the generating functional of *full* Green functions. We can derive expectation values of full n -point correlation functions for either fermionic or bosonic fields φ^i by differentiating with respect to the sources:

$$\langle \varphi^1 \varphi^2 \dots \rangle := \frac{\delta}{\delta \eta^1} \frac{\delta}{\delta \eta^2} \dots Z[\eta]. \quad (2)$$

These correlation functions are in general dependent on non-zero sources. To obtain the full n -point Green function, the vacuum expectation value is to be calculated by setting the sources η to zero and making use of the normalization $Z[0] = 1$. This also implies setting $\langle \varphi^i \rangle|_{\eta=0} \equiv 0 \forall i$ because of translational invariance of the vacuum¹. The derivatives in (2) are ordinary functional left derivatives if with respect to bosonic fields or their sources. For fermionic fields, derivatives w.r.t. $\bar{\varphi}_F^i$ are also left derivatives, but in order to circumvent explicit minus signs, derivatives w.r.t. φ_F^i are right derivatives by definition:

$$\frac{\delta}{\delta \varphi_F^i} := \overleftarrow{\delta} \quad , \quad \frac{\delta}{\delta \eta_F^i} := \overleftarrow{\delta}. \quad (3)$$

To arrive at the *connected* Green functions, one defines their generating functional by

$$W[\eta] = \ln Z[\eta] \quad (4)$$

such that for fields φ^i

$$\langle \varphi^1 \varphi^2 \dots \rangle_{conn.} := \frac{\delta}{\delta \eta_1} \frac{\delta}{\delta \eta_2} \dots W[\eta]. \quad (5)$$

With these definitions, the full n -point correlation functions can be decomposed into connected ones. An intuitive explanation for the terminology is provided here when realizing that the full correlation functions are linear combinations of products of connected Green function and disconnected vacuum bubbles given by $Z[\eta]$. The decomposition yields

$$\langle \varphi^1 \rangle = \langle \varphi^1 \rangle_{conn.} Z[\eta], \quad (6)$$

$$\langle \varphi^1 \varphi^2 \rangle = \langle \varphi^1 \varphi^2 \rangle_{conn.} Z[\eta] + \langle \varphi^1 \rangle_{conn.} \langle \varphi^2 \rangle_{conn.} Z[\eta], \quad (7)$$

$$\begin{aligned} \langle \varphi^1 \varphi^2 \varphi^3 \rangle &= \langle \varphi^1 \varphi^2 \varphi^3 \rangle_{conn.} Z[\eta] + \langle \varphi^1 \varphi^2 \rangle_{conn.} \langle \varphi^3 \rangle_{conn.} Z[\eta] + \langle \varphi^2 \varphi^3 \rangle_{conn.} \langle \varphi^1 \rangle_{conn.} Z[\eta] \\ &\quad + \langle \varphi^3 \varphi^1 \rangle_{conn.} \langle \varphi^2 \rangle_{conn.} Z[\eta] + \langle \varphi^1 \rangle_{conn.} \langle \varphi^3 \rangle_{conn.} \langle \varphi^3 \rangle_{conn.} Z[\eta], \end{aligned} \quad (8)$$

One can directly see here that the vacuum expectation values of full and connected 3-point Green functions are equivalent, but they are not for 4-point Green functions:

$$\langle \varphi^1 \varphi^2 \varphi^3 \varphi^4 \rangle|_{\eta=0} = \left(\langle \varphi^1 \varphi^2 \varphi^3 \varphi^4 \rangle_{conn.} + \sum_{k \neq l \neq m \neq n} (\pm)^{klmn} \langle \varphi^k \varphi^l \rangle_{conn.} \langle \varphi^m \varphi^n \rangle_{conn.} \right) \Big|_{\eta=0}. \quad (9)$$

¹It is assumed that the symmetry of the vacuum is unbroken.

The \pm indicates that for Grassmannian fields φ_F and $\bar{\varphi}_F$ one has to take feasible anticommutations into account. The generating functional of *proper*² Green functions is defined as the Legendre transform of $W[\eta]$ with respect to all fields, known as the *effective action* Γ :

$$\Gamma[\varphi] = -W[\eta] + \varphi_B^i \eta_B^i + \bar{\varphi}_F^i \eta_F^i + \bar{\eta}_F^i \varphi_F^i \quad (10)$$

By this definition, fields and sources are linked by

$$\frac{\delta W}{\delta \eta^i} = \varphi^i \quad , \quad \frac{\delta \Gamma}{\delta \varphi^i} = \eta^i \quad . \quad (11)$$

such that their derivatives can be associated by

$$\frac{\delta}{\delta \varphi^i} = \frac{\delta^2 \Gamma}{\delta \varphi^i \delta \varphi^j} \frac{\delta}{\delta \eta^j} \quad , \quad \frac{\delta}{\delta \eta^i} = \frac{\delta^2 W}{\delta \eta^i \delta \eta^j} \frac{\delta}{\delta \varphi^j} \quad . \quad (12)$$

So if the derivatives w.r.t. fields are to (anti)commute, and the derivatives w.r.t. the sources are to (anti)commute as well, then consequently derivatives w.r.t. fields will not (anti)commute with derivatives w.r.t. the sources.

The procedure which was just introduced bears an astonishing analogy to information theory (or equally statistical mechanics) where the expectation values are obtained by derivatives of the partition sum with respect to the Lagrange parameters [Fel02]. These parameters constrain the outcome of the calculation by enforcing known expectation values of the observables of the theory. The counterparts of the Lagrange parameters are here the sources which give us insight into the radiative corrections. The analogy now allows us to understand that setting the sources to zero at the end of the calculation is nothing but to say that the expectation values of the fields were not known in the first place.

2.2 Yang-Mills theories

$SU(N_c)$ Yang-Mills theories [Yan54] describe the dynamics of $N_c^2 - 1$ gauge particles which transform in the adjoint representation of the symmetry group. QCD is formulated as a $SU(3)$ theory where there are also $N_c = 3$ quarks transforming in the fundamental representation. The influence of quarks is, however, assumed to cause only minor effects on the dynamics of the gauge sector [Fis03]. Therefore, QCD is here approximated by a $SU(3)$ YM theory. Generalizing to $SU(N_c)$, the classical Yang-Mills theories are governed by the following Euclidian Lagrangian:

$$\mathcal{L} = \frac{1}{4} (F_{\mu\nu}^a)^2 \quad (13)$$

It involves the field strength tensor $F_{\mu\nu}^a$ which is the kinetic part of the gluon fields A_μ^a with color index a and a term which describes self-interaction among them,

$$F_{\mu\nu}^a = \partial_\mu A_\nu^a - \partial_\nu A_\mu^a - g_d f^{abc} A_\mu^b A_\nu^c \quad . \quad (14)$$

²also known as *one-particle irreducible* (1PI)

The mass dimension of the coupling g_d depends on the spacetime dimension d . The self-interaction occurs only in theories in which the structure constants f^{abc} are non-zero, i.e. in non-Abelian gauge theories. The structure constants are specific to the gauge group and obey certain identities that are noted in appendix A.2. The non-Abelian nature of the theory we intend to describe requires the covariant derivative of the gauge fields in the adjoint representation to obey

$$D_\mu^{ab} = \delta^{ab} \partial_\mu + g_d f^{abc} A_\mu^c. \quad (15)$$

The theory described by (13) is invariant under gauge transformations. The gauge symmetry is generated by first-class constraints Φ^a implicit in the the Lagrangian by means of Poisson brackets with the gauge fields [Dir64, Hen92]. We thus find a configuration space of the gauge fields $A \equiv \{A^a\}$, in which the physics is equivalent. Along the orbits of infinitesimal gauge transformations,

$$A_\mu^a \longrightarrow A_\mu^a - \partial_\mu \alpha^a - f^{abc} A_\mu^b \alpha^c, \quad (16)$$

the Lagrangian (13) is invariant for any $\alpha(x)$. One possibility to avoid ambiguities³ in the S matrix (which is to be gauge invariant) is to choose gauge-fixing conditions $\chi^b(A) = 0$ which cut the configuration space and remove the freedom of transformations of the gauge fields. If the gauge-fixing condition is not to cut the configuration space locally twice, we have to demand that it is left invariant under the gauge transformations for a unique $\alpha(x)$. This is assured by requiring that $\det(\{\Phi^a, \chi^b\}_P) \neq 0$ where $\{\cdot, \cdot\}_P$ is the Poisson bracket. The linear covariant gauge fixing condition to choose is $\chi^a(A) = \partial_\mu A_\mu^a = 0$, called Lorentz gauge.

Quantizing the theory in the path integral formalism (see, e.g., [Pes95]), the gauge-fixing condition is implemented as a delta function in the integrand of the gauge space. The integration is then performed over the given hypersurface of gauge fields. One can show that by requiring

$$\det(-\partial_\mu D_\mu^{ab}) \neq 0 \quad (17)$$

the gauge-fixing procedure is locally unique for infinitesimally neighboring configurations. This does not remove the possibility of large gauge transformations leading to Gribov copies [Gri78]. We shall not discuss these ambiguities here.

In the path integral over gauge fields, the Lorentz gauge-fixing condition is smeared out by exponentiation to a Gaussian distribution of width ξ

$$\delta(\partial_\mu A_\mu^a) \longrightarrow \exp\left(-\frac{1}{2\xi} \int \bar{d}^d x (\partial_\mu A_\mu^a(x))^2\right) \quad (18)$$

This effectively introduces another term in the Lagrangian with ξ as a new parameter, the *gauge parameter*, that can be freely chosen. The *Landau gauge*, where $\xi = 0$, plays

³These are circumvented in stochastic quantization and lattice theory.

a distinct role in the gauge-fixing procedure as well as in this work, see section 2.3. It enforces the Lorentz gauge with an infinite weight in (18) and thereby ensures that even quantum fluctuations will obey the condition $\partial_\mu A_\mu^a = 0$. In particular, this means that the gauge propagator will be transverse in the Landau gauge [Alk01].

In the quantization of the theory, Faddeev and Popov [Fad67] used a trick of rewriting the determinant (17) as a Gaussian integral over Grassmann valued scalar fields giving rise to the so-called *Faddeev-Popov ghosts* which are namely the ghost fields c^a and the antighost fields \bar{c}^a ,

$$\det(-\partial_\mu D_\mu^{ab}) = \exp \left(\int d^d x \bar{c}^a \partial_\mu D_\mu^{ab} c^b \right). \quad (19)$$

Since the ghosts do not have the correct relation between spin and statistics they cannot be asymptotic states.⁴ They do, however, serve as negative degrees of freedom to cancel unphysical longitudinal polarizations of the gluons, and are therefore crucial to preserve unitarity. Also, the confinement mechanism is understood to be due to ghost field contributions, see section 4.3.

Although in general covariant gauges, the ghost and the antighost fields are independent fields, in the Landau gauge one obtains a ghost-antighost symmetry (cf. section 5.2) assigning $c^\dagger \equiv \bar{c}$ for complex fields. For general covariant gauges, this hermiticity assignment leads to a Lagrangian that is neither strictly hermitian nor compatible with BRS transformations [Nak90] and can be used only at the expense of quartic ghost interactions. For the Landau gauge, however, which is the gauge mainly used in this work, quartic ghost interactions do not contribute and we may use the above hermiticity assignment if we take the limit $\xi \rightarrow 0$ at the end of the calculations [Alk01].

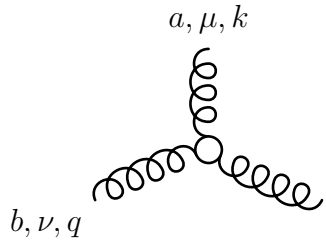
For the derivation of quantized correlation functions, the gauge-fixed path integral reads

$$\begin{aligned} Z[J, \bar{\sigma}, \sigma] = & \int \mathcal{D}[A\bar{c}c] \exp \left\{ - \int d^d x \left(\frac{1}{4} (F_{\mu\nu}^a)^2 + \frac{1}{2\xi} (\partial_\mu A_\mu^a)^2 + \bar{c}^a \partial_\mu D_\mu^{ab} c^b \right) \right. \\ & \left. + \int d^d x (A^a J^a + \bar{\sigma}^a c^a + \bar{c}^a \sigma^a) \right\}, \end{aligned} \quad (20)$$

where J_μ^a , $\bar{\sigma}^a$ and σ^a were introduced as sources for the fields A_μ^a , c^a and \bar{c}^a , respectively.

Although the Green functions defined in this theory are gauge dependent, their generating functional given by eq. (20) is independent of the gauge-fixing condition chosen. This is reflected in an underlying symmetry of the gauge-fixed quantized Lagrangian called *Becchi-Rouet-Stora (BRS) symmetry* [Bec75]. In the same way as the gauge symmetry appears in the classical Lagrangian which can be connected to charge conservation, the BRS symmetry is found in the gauge-fixed quantized Lagrangian. BRS symmetry can be seen as a set of constraints on the gauge independent generating functional that couples the gauge

⁴The absence of ghost fields from the S matrix can also be understood in the context of BRS symmetry [Nak90].



$$\equiv \Gamma_{\mu\nu\rho}^{abc}(k, q, p) = (2\pi)^d \delta^{(d)}(k + q + p) g_d f^{abc} \Gamma_{\mu\nu\rho}(k, q, p). \quad (24)$$

Again, the color structure is assumed to comply with perturbation theory and it has been extracted from the vertices along with the momentum conservation and the gauge coupling in (23) and (24) to define the more succinct reduced vertices $\Gamma_\mu(k; q, p)$ and $\Gamma_{\mu\nu\rho}(k, q, p)$. In the bare form these are found to be

$$\Gamma_\mu^{(0)}(q) = iq_\mu, \quad (25)$$

$$\Gamma_{\mu\nu\rho}^{(0)}(k, q, p) = -i(k - q)_\rho \delta_{\mu\nu} - i(q - p)_\mu \delta_{\nu\rho} - i(p - k)_\nu \delta_{\mu\rho}, \quad (26)$$

which can be directly obtained by applying derivatives to the action $\mathcal{S} = \int d^d x \mathcal{L}$ of the theory with respect to the fields involved in the vertices.

2.3 Landau gauge

For the study of gauge-dependent Green functions, one is free to choose a gauge parameter ξ . The covariant gauge which has been picked for this and also related calculations is the Landau gauge, where $\xi = 0$, the reason being that the complexity of a non-perturbative treatment reduces considerably as will be discussed in the following. The propagators, in particular, have been calculated in the Landau gauge, see section 4. There, this choice eliminates the influence of the four-ghost vertex as well as the tadpole. The Landau gauge also plays a distinctive role for renormalization in the sense that the gauge parameter ξ need not be renormalized. Any multiplicative renormalization constant will not alter $\xi = 0$. In this sense, the Landau gauge forms a fixed point in the renormalization group. Furthermore, the running coupling can be formulated in terms of the propagators in this gauge, see sec. 6.2. Most importantly, the Landau gauge provides first principle constraints for the ghost-gluon vertex and thus alleviates a non-perturbative approach on the Green functions of the theory. These constraints shall be presented now.

It was shown in [Mar78, Tay71] that in the Landau gauge the proper ghost-gluon vertex must reduce to its tree-level form if one takes the limit of the incoming ghost momentum p to zero,

$$\lim_{p \rightarrow 0} \Gamma_\mu(k; q, p) = \Gamma_\mu^{(0)}(q). \quad (27)$$

This general statement is a crucial guideline for the constructions of the ghost-gluon vertex to be made. Taking a look at the renormalization of the vertex, one can define the renormalization constant \tilde{Z}_1 of the ghost-gluon vertex by

$$\Gamma_\mu \longrightarrow \Gamma_\mu^R \equiv \tilde{Z}_1 \Gamma_\mu^{(0)}, \quad (28)$$

assuming multiplicative renormalizability of the non-perturbative vertex. Due to the identity (27) \tilde{Z}_1 can be fixed to a finite constant. If the renormalization point is chosen either in the infrared or in the asymptotic ultraviolet, one gets

$$\tilde{Z}_1 = 1. \tag{29}$$

This result called *non-renormalization* was first shown in [Tay71] as a Slavnov-Taylor identity and leads us to the conclusion that in the ultraviolet regime of the vertex the leading asymptotic behavior can be expected. Generally speaking, the Landau gauge turns out to be a gauge that is less divergent than other gauges.

3 Dyson-Schwinger equations

The Dyson-Schwinger equations may be regarded as the pivot of the study of YM theories in this and related works. Therefore, the derivation will be formally presented here. The need and the realization of a truncation will be discussed and the truncated DSEs for the propagators as well as the ghost-gluon vertex will be calculated.

3.1 Derivation of Dyson-Schwinger equations

The derivation of DSEs can be found in a number of textbooks, such as [Bjo65] and [Itz80]. Both the operator formalism as well as the functional integral formalism are possible frameworks. For the purposes of examining Yang-Mills theories, the functional integral method will be used. A lucid treatment of this approach to derive DSEs can be found in [Rob94]. The crucial idea of the procedure is based on the fact that a functional integral over a total derivative vanishes. This holds true only if [Riv87]

- the measure $\mathcal{D}\varphi$ is invariant under field transformations of the form $\varphi(x) \rightarrow \varphi(x) + \Lambda(x)$ for arbitrary $\Lambda(x)$,
- the representation of the generating functional as given in (1) exists.

The former is reminiscent of the derivation of the classical Euler-Lagrange equations where the action is required to be invariant under infinitesimal variations of the fields. Nonetheless, no way has been found to prove either of the above conditions and they shall be assumed henceforth.

One may start with a derivative with respect to the field $\bar{\varphi}_F^k$ to find

$$\begin{aligned}
 0 &= \int \mathcal{D}[\varphi] \frac{\delta}{\delta \bar{\varphi}_F^k} \exp(-\mathcal{S}[\varphi] + \varphi_B^i \eta_B^i + \bar{\varphi}_F^i \eta_F^i + \bar{\eta}_F^i \varphi_F^i) \\
 &= \int \mathcal{D}[\varphi] \left(-\frac{\delta \mathcal{S}[\varphi]}{\delta \bar{\varphi}_F^k} + \eta_F^k \right) \exp(-\mathcal{S}[\varphi] + \varphi_B^i \eta_B^i + \bar{\varphi}_F^i \eta_F^i + \bar{\eta}_F^i \varphi_F^i) \\
 &= \left(-\frac{\delta \mathcal{S} \left[\frac{\delta}{\delta \eta} \right]}{\delta \bar{\varphi}_F^k} + \eta_F^k \right) Z[\eta] = \left\langle -\frac{\delta \mathcal{S}[\varphi]}{\delta \bar{\varphi}_F^k} + \eta_F^k \right\rangle
 \end{aligned} \tag{30}$$

The DSE for a n -point Green function now follow from successive derivation w.r.t. the sources of whichever fields are of interest. It is important to maintain non-zero sources until all derivatives are performed in order not to neglect any terms. Eventually only the vacuum expectation values that depend on pairs of Grassmann fields remain, others are zero because the bosonic functionals $W[\eta]$ and $\Gamma[\varphi]$ can depend on pairs of Grassmann fields only. For example, it can be easily seen that the following quantity must vanish:

$$\frac{\delta^2 \Gamma}{\delta \varphi_F^k \delta \varphi_F^k} = -\frac{\delta^2 \Gamma}{\delta \varphi_F^k \delta \varphi_F^k} = 0. \tag{31}$$

One can also argue that the conservation laws lead to the same conclusions. If, for example, a Green function involves Faddeev-Popov-ghosts, it can only depend on pairs of ghost and antighost fields, otherwise the ghost number would not be conserved.

The n -point Green functions obtained in this way can be formally⁶ expressed as

$$\left\langle \prod_{i=1}^m \varphi^i \frac{\delta \mathcal{S}}{\delta \varphi^k} \right\rangle \Big|_{\eta=0} = \sum_{j=1}^m \left\langle \prod_{i \neq j} \varphi^i \delta^{jk} \right\rangle \Big|_{\eta=0}, \tag{32}$$

where the right hand side represents the quantum effects, so called *contact terms*, that contribute where two fields coincide. The DSEs given by eq. (32) are often referred to as the quantum equations of motion for Green functions due to their connection to the classical Euler-Lagrange equations of motion via the identity

$$\frac{\delta \mathcal{S}[\varphi]}{\delta \varphi^k} = \frac{\partial \mathcal{L}}{\partial \varphi^k} - \partial_\mu \left(\frac{\partial \mathcal{L}}{\partial (\partial_\mu \varphi^k)} \right). \tag{33}$$

Evidently, the quantum equations of motion satisfy the classical equation of motion up to contact terms arising from commutation relations of field operators.

⁶For simplicity, feasible Grassmannian nature of fields is discarded here. Taking them into account will involve extra minus signs.

3.2 Truncation

The set of equations (32) derived in the Dyson-Schwinger formalism is an infinite tower of non-linear coupled equations. To solve for one particular n -point Green function, the $(n + 1)$ -point functions (and possibly more) have to be computed. Due to this recursive coupling which makes one Green function dependent on all the others, a decoupling of a subset of the equations is necessary to be able to approximately solve it⁷. In particular this means that some of the n -point functions have to be neglected. For example, the decoupling of a set of equations involving the 2-point and 3-point Green functions can be achieved by neglecting all $(n \geq 4)$ -point functions and thus *truncating* a part of the whole set of DSEs as given in (32). This specific truncation has been developed to solve the DSEs for the ghost and gluon propagators in [Sme98b], see section 4. In the next section, the DSEs will be presented within this truncation scheme.

Truncations which lead to soluble subsets of equations generally break gauge invariance explicitly and one has to check the extent of the violation to be able to assess a posteriori if the truncation is a useful approximation. The truncation developed in [Sme98b] for the calculation of the ghost- and the gluon propagator, has proven to be reasonable in this respect [Fis02].

3.3 Dyson-Schwinger equations for the ghost- and gluon propagator

Following the outline of section 3.1, the DSEs for the ghost- and gluon propagators can be derived in a straightforward but tedious calculation. The main steps for the derivation of the ghost DSE, although not all, are performed in appendix B. In momentum space, one arrives at

$$[D_G(p)]^{-1} = [D_G^{(0)}(p)]^{-1} - g_d^2 N_c \int \bar{d}^d q \Gamma_\mu(q; p - q, p) D_{\mu\nu}(q) \Gamma_\nu^{(0)}(p) D_G(p - q). \quad (34)$$

The trivial color indices of the propagators have been suppressed. This involves rendering equal the color structures of bare and proper vertices and contracting them to yield the factor N_c , see eq. (72) in the appendix.

The DSE for the gluon propagator neglecting any 4-point functions reads

$$\begin{aligned} [D(p)]_{\mu\nu}^{-1} &= [D^{(0)}(p)]_{\mu\nu}^{-1} + g_d^2 N_c \int \bar{d}^d q \Gamma_\mu^{(0)}(q - p) D_G(q - p) \Gamma_\nu(-p; q, q - p) D_G(q) \\ &\quad - \frac{1}{2} g_d^2 N_c \int \bar{d}^d q \Gamma_{\mu\rho\sigma}^{(0)}(p, -q, q - p) D_{\rho\rho'}(q) \Gamma_{\nu\sigma'\rho'}(-p, p - q, q) D_{\sigma\sigma'}(q - p). \end{aligned} \quad (35)$$

The graphical representations of these DSEs are depicted in fig. 1.

⁷It is possible to make a series expansion that leads to the Feynman diagrams.

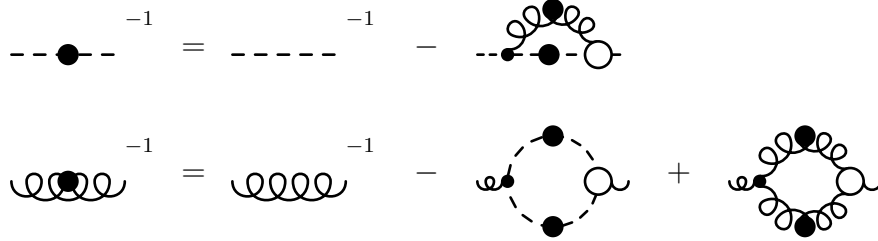


Figure 1: The truncated set of DSE's for the gluon and for the ghost propagator. Wiggly lines with filled blobs represent connected gluon propagators, without blobs bare propagators. Ghost propagators are equivalently denoted by dashed lines. Vertices with empty blobs represent proper vertices, small dots represent bare vertices.

3.4 Dyson-Schwinger equation for the ghost-gluon vertex

The derivation of the DSE for the ghost-gluon vertex without any truncations has been performed and can be looked up in appendix B. According to the truncation applied to the propagators, the vertex DSE is presented here excluding the four-point interaction. The identity (27) which follows from first principle is not violated by this neglect since it can be shown analytically that the term which implicates the four-point interaction vanishes in the infrared limit of incoming ghost momentum⁸. Also, it vanishes perturbatively and therefore would not influence the ultraviolet behavior of the vertex.

The DSE for the ghost-gluon vertex, the graphical representation of which can be seen in fig. 2, then reads

$$\begin{aligned}
 \Gamma_\mu(k; q, p) &= \Gamma_\mu^{(0)}(k; q, p) \\
 &\quad - \frac{1}{2} g_d^2 N_c \int \bar{d}^d \omega \Gamma_\mu(k; \omega, \omega + k) \\
 &\quad \quad \times D_G(\omega) \Gamma_\nu^{(0)}(q) D_{\nu\lambda}(\omega - q) \Gamma_\lambda(q - \omega; \omega + k, p) D_G(\omega + k) \\
 &\quad - \frac{1}{2} g_d^2 N_c \int \bar{d}^d \omega \Gamma_{\mu\nu\rho}(k, \omega, \omega + k) \\
 &\quad \quad \times D_{\nu\lambda}(\omega) \Gamma_\lambda^{(0)}(q) D_G(\omega - q) \Gamma_\sigma(q - \omega; \omega + k, p) D_{\rho\sigma}(\omega + k), \quad (36)
 \end{aligned}$$

where the suppressed color structure of the vertices and propagators has been contracted according to eq. (73) in appendix A.2 to yield the factors $-\frac{1}{2} N_c$.

⁸This can be proven equivalently to the argument for the reduction to the bare vertex in [Tay71].

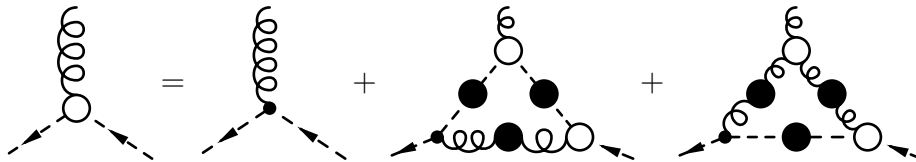


Figure 2: Truncated DSE for the ghost-gluon vertex

4 Propagators of Yang-Mills theory

The truncation of the subset of DSEs for the propagators of Yang-Mills theory as it was demonstrated in section 3.2 was first developed in [Sme97]. All four-point functions are discarded up to one exception, the tadpole diagram of the gluon DSE⁹. The neglect of the other diagrams with four-point interactions (which are all two-loop diagrams) is known not to affect the infrared behavior of the propagators [Vac95], in the ultraviolet they are subleading due to asymptotic freedom. For intermediate momenta, the inclusion of two-loop terms may comply with lattice results if considerable effort is put into constructing a suitable truncation [Blo03]. Further approximations have been employed to arrive at an iterative solution of the results. In this section, these approximations will be mentioned and the results as well as their interpretation will be discussed. For the calculation of the ghost-gluon vertex in section 6, the results of the propagators will be crucial.

4.1 Vertex approximations

The truncated DSEs for the ghost- and gluon propagators as they are depicted in fig. 1 are still very hard to solve self-consistently when coupled to the DSEs for the vertices. An iteration would have to be performed for all the equations simultaneously. In order to circumvent these technical difficulties, ansätze have been made for the vertices to succeed in obtaining a self-consistent solution for the propagators [Fis02, Maa04].

For the ghost-gluon vertex, one applies a *bare vertex approximation*. This is an estimate that is motivated, on the one hand, by the non-renormalization of this vertex in the Landau gauge whence no divergences are expected to emerge in the ultraviolet. In the infrared limit, on the other hand, the Slavnov-Taylor identity tells us that the vertex is bare for a vanishing incoming ghost-momentum. In addition, Zwanziger's hypothesis (see section 5.3) indicates that even for the infrared limit of the gluon momentum the vertex reduces to tree-level. Therefore, one is tempted to assume that the bare vertex is a good approximation for the whole range of momenta. One of the main motivations for the investigations of the ghost-gluon vertex in this work is to clarify whether or not the bare vertex approximation is justified.

⁹The tadpole was retained since it produces merely a constant.

The three-gluon vertex for $d = 4$ is chosen [Fis02] in such a way that the propagators obtain the correct anomalous dimensions from leading-order perturbation theory at short distances. For $d = 3$ a construction is made [Maa04] avoiding additional breaking of gauge invariance which would occur in the gluon loop of the gluon propagator if one chose the three-gluon vertex to be bare.

4.2 Previous results

The results for the propagators obtained with the bare vertex approximation for the ghost-gluon vertex and a construction for the three-gluon vertex as they were obtained for three dimensions in [Maa04] and for four dimensions in [Fis02] will be displayed here and employed for the study of the ghost-gluon vertex later on. The solution solves the truncated DSEs self-consistently. In figs. 3 and 4 the results are plotted in comparison to lattice results.

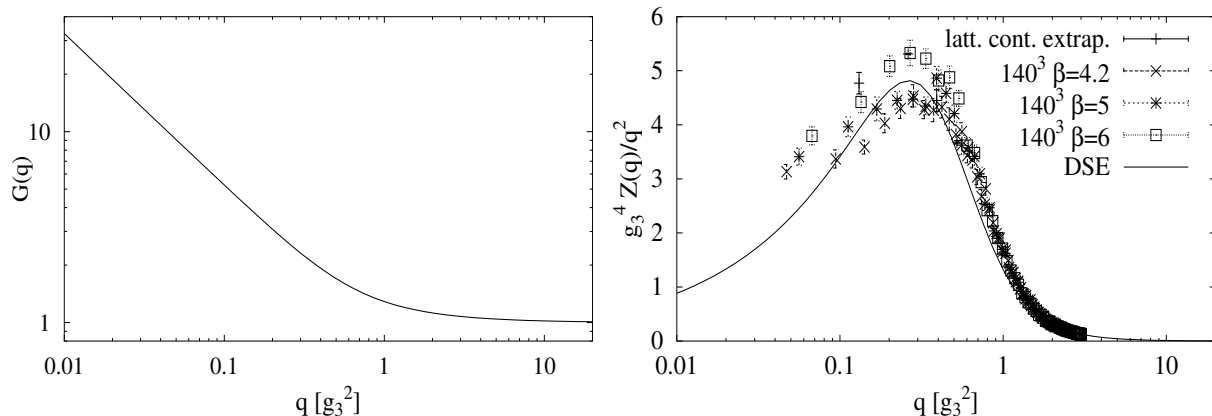


Figure 3: The $d = 3$ results from DSEs [Maa04] for the ghost dressing function (left) and the gluon propagator (right) compared to lattice calculations [Cuc01, Cuc03]. g_3 is the coupling constant with a mass dimension in three-dimensional Yang-Mills theory.

Both for three and for four dimensions the propagators show the same qualitative behavior. The ghost propagator shows an enhancement stronger than $1/p^2$ in the infrared whereas the gluon propagator is suppressed in the infrared. The infrared suppression is found to be due to the ghost loop in the gluon DSE [Sme97]. A good agreement is found in the comparison with lattice results, the largest deviation is present for intermediate momenta. Due to finite volume effects of the lattice, the infrared behavior lacks lattice data, this shortcoming in lattice theory has the counterpart of the necessity of a truncation in DSE studies.

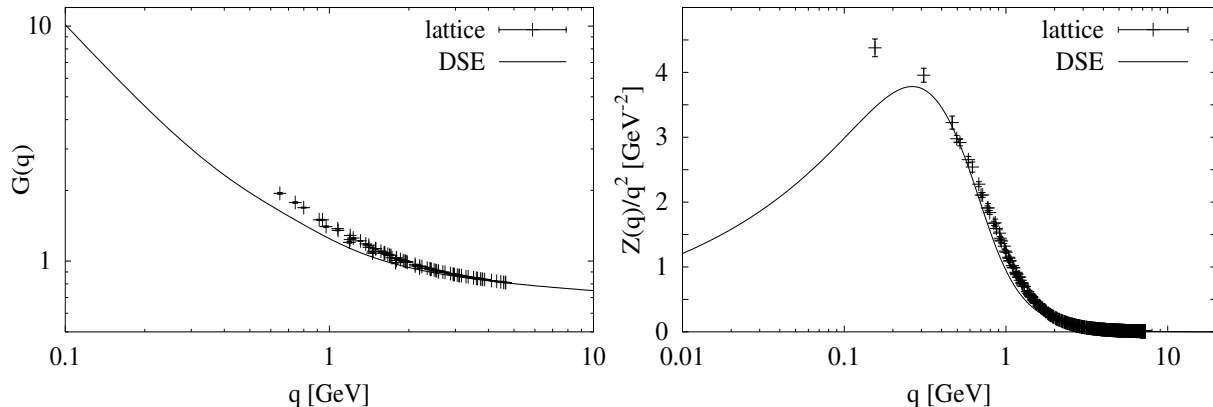


Figure 4: The $d = 4$ results from DSEs [Fis02] for the ghost dressing function (left) compared to lattice calculations [Lan02] and the gluon propagator (right) with lattice results from [Bow04]. Mind that the lattice data at low momenta are likely to be strongly influenced by finite volume effects.

4.3 Implications for gluon confinement

Confinement is a phenomenon mediated by long-range interactions (i.e., at the order of the size of a hadron), so the infrared behavior of the Green functions is of particular interest. For the ghost field a confining mechanism is redundant since the ghost propagator does not appear in the S matrix a priori [Pes95]. Its infrared enhancement, however, is the leading contribution to the infrared suppression of the gluon propagator. A propagator which vanishes in the infrared cannot have a Källén-Lehmann spectral representation because it violates positivity and therefore must be confined [Alk04a]. Thus, gluons are confined by long-range interactions that are mediated by ghosts. This intuitive picture can be put briefly by saying: the ghosts are confining and the gluons are confined.

More sophisticated scenarios for confinement in the Landau gauge are namely the Kugo-Ojima confinement criterion [Kug79, Kug95] or the Zwanziger-Gribov condition [Zwa04, Zwa94, Gri78]. Both scenarios request an infrared enhancement of the ghost propagator such as it was found in the calculations. In Coulomb gauge a complementary picture of confinement is found which relates the infrared enhancement to center vortices and the Gribov horizon, see [Feu04, Gre04].

One outstanding feature of the results is that the three-dimensional calculations which describe the theory in the asymptotic high-temperature limit do not show significant deviations from the four-dimensional vacuum theory [Maa04]. This indicates that the notion of “deconfinement” in the QCD phase diagram as it was suggested originally in the context of the quark-gluon plasma has to be revised. Findings in lattice theory [Lae03] also show that there are considerable deviations in the equation of state from a Boltzmann gas suggested for the “deconfined” phase. Thus these investigations point at remnant interactions in the

high-temperature phase.

5 Analytical structure of the ghost-gluon vertex

In this section, the calculation of the ghost-gluon vertex will be implemented as an iterative solution of the DSE given by eq. (36). Formulae are derived for performing one iteration step both perturbatively and non-perturbatively in the next section. The four-point function which contributes to the vertex DSE, see appendix B, is discarded in compliance with the truncation of the DSEs for the propagators. As starting points for the iteration to be inserted into the right hand side of eq. (36) the bare as well as a STI-motivated ghost-gluon vertex will be considered. An ansatz has to be made for the three-gluon vertex involved in the DSE of the ghost-gluon vertex. Since the three-gluon vertex is assumed to be subdominant in the infrared [Alk01], the ansatz is chosen to be at tree-level. Recently [Alk04b] there have been indications that in order to find a self-consistent solution for the quark propagator in DSE studies of QCD, the three-gluon vertex ought to be singular in the infrared. Therefore, a further investigation might be mandatory to approximate QCD. In particular, one might employ a STI-motivated ansatz for the three-gluon vertex such as the construction in [Alk01]. However, in order to calculate the Green functions of pure YM-theory, the bare three-gluon vertex will be used here as an ansatz.

In addition to the Lorentz structure of the vertex, its symmetry properties as well as implications for its infrared behavior from the STI will be discussed.

5.1 Lorentz structure

In a Lorentz invariant theory, the ghost-gluon vertex must transform as a vector in the Lorentz group. Therefore, it must depend on the momenta in a Lorentz covariant way and decompose to

$$\Gamma_\mu(k; q, p) = iq_\mu(1 + A(k^2; q^2, p^2)) + ik_\mu B(k^2; q^2, p^2), \quad (37)$$

where $A(k^2; q^2, p^2)$ and $B(k^2; q^2, p^2)$ are scalar functions to be determined from the form of the vertex given in eq. (36). In order to initiate the iteration with the bare ghost-gluon vertex as a starting point, the vertices in the integrand are replaced by their tree-level forms. The first step is to perform the contractions in the kernel. A helpful tool for doing so is FORM [Ver00]. The resulting vector integrals have one or two external scales and can be reduced to scalar integrals using the techniques outlined in appendix C.1. The algorithm for extracting Lorentz structure from general tensor integrals is given by ref. [Pas79]. One then obtains in arbitrary dimension and covariant gauge

$$\begin{aligned}
 A(k^2; q^2, p^2)|_{\text{bare input}} &= \frac{g_d^2 N_c}{2\Delta} \int \bar{d}^d \omega \left\{ \frac{G(\omega^2)G((\omega+k)^2)}{\omega^2(\omega-q)^4(\omega+k)^2} (Z((\omega-q)^2)A_1 + \xi A_3) \right. \\
 &\quad + \frac{G((\omega-q)^2)}{\omega^4((\omega-q)^2)^2(\omega+k)^4} (Z(\omega^2)Z((\omega+k)^2)A_2 \\
 &\quad \left. + Z((\omega+k)^2)\xi A_4 + Z(\omega^2)\xi A_5 + \xi^2 A_6) \right\} , \tag{38a}
 \end{aligned}$$

$$\begin{aligned}
 B(k^2; q^2, p^2)|_{\text{bare input}} &= \frac{g_d^2 N_c}{2\Delta} \int \bar{d}^d \omega \left\{ \frac{G(\omega^2)G((\omega+k)^2)}{\omega^2(\omega-q)^4(\omega+k)^2} (Z((\omega-q)^2)B_1 + \xi B_3) \right. \\
 &\quad + \frac{G((\omega-q)^2)}{\omega^4(\omega-q)^2(\omega+k)^4} (Z(\omega^2)Z((\omega+k)^2)B_2 \\
 &\quad \left. + Z((\omega+k)^2)\xi B_4 + Z(\omega^2)\xi B_5 + \xi^2 B_6) \right\} , \tag{38b}
 \end{aligned}$$

where $\Delta = q^2 k^2 - (q \cdot k)^2$ is the Gram determinant and the functions A_1 through A_6 and B_1 through B_6 are quoted in appendix D. In the Landau gauge, only the kernels A_1 , A_2 , B_1 and B_2 are relevant. It therefore incorporates a considerable simplification for the computational effort. Moreover, the longitudinal part of the vertex, determined by the function B , is mostly irrelevant in the Landau gauge. If contracted with a gluon propagator, the vertex will be fully determined by its transverse projection,

$$\frac{k^2}{ig_d \Delta} q_\mu t_{\mu\nu}(k) \Gamma_\nu(k; q, p) = 1 + A(k; q, p) , \tag{39}$$

where all contributions from B vanish. Therefore, the function A is the object to be focused on for most purposes.

5.2 Symmetry

For the Landau gauge, the gauge fixing condition $\partial_\mu A_\mu = 0$ of covariant gauges is strictly enforced, also for quantum fluctuations. I.e. , the derivatives in the Faddeev-Popov determinant commute, $[\partial_\mu, D_\mu] = 0$, and one is free to choose in which order one will write the determinant by virtue of a Grassmann integral. The resulting ghost-antighost conjugation leads to the symmetry [Sme98b]

$$A(k^2; q^2, p^2) = A(k^2; p^2, q^2) \tag{40}$$

which can be shown explicitly on the level of the integrand to be fulfilled only in the Landau gauge¹⁰. It was shown in [Ler02] that in the manifestly ghost-antighost symmetric Landau gauge, the whole ghost-gluon vertex will acquire a symmetry in the ghost momenta such that $\Gamma_\mu(k; q, p) = \Gamma_\mu(k; p, q)$. In this case, in addition to (40) the function $B - (1+A)/2$

¹⁰This has been done but will not be displayed for it is rather technical.

would be antisymmetric in the ghost momenta. However, since here we input a tree-level vertex which is not ghost-antighost symmetric, the whole vertex cannot be symmetric either.

5.3 Slavnov-Taylor identity

Taking into consideration a STI for the ghost-gluon vertex, the infrared limit of the vertex can be partly kept under control. The results of the calculations to come are required to satisfy the STI in order to not break gauge invariance. Furthermore, the vertex STI has motivated additional ansätze for the vertex, one of which will be presented here and investigated in the next section as another potential candidate for the non-perturbative ghost-gluon vertex.

If one applies the BRS variation δ_{BRS} to a suitable correlation function,

$$0 = \delta_{BRS} \langle c^a \bar{c}^b \bar{c}^c \rangle , \quad (41)$$

it can be shown [Sme98b] that one arrives at a STI for the ghost-gluon vertex. Given the present truncation neglecting all four-point functions, it reads

$$ik_\mu G^{-1}(k^2) \Gamma_\mu(k; q, p) - ip_\mu G^{-1}(p^2) \Gamma_\mu(-p; q, -k) = \tilde{Z}_1 q^2 G^{-1}(q^2) . \quad (42)$$

This equation holds true for any gauge parameter ξ . The reduction to the bare vertex given by eq. (27), valid without truncation but only for $\xi = 0$ (see section 2.3), is reproduced by the STI (42) in the following way. For $p \rightarrow 0$ one has $k \rightarrow -q$ and finds with $\lim_{p \rightarrow 0} p^2 G^{-1}(p^2) = 0$:

$$-iq_\mu \Gamma_\mu(k; q, 0) = \tilde{Z}_1 q^2 \quad \iff \quad \Gamma_\mu(k; q, 0) = \tilde{Z}_1 \Gamma_\mu^{(0)}(q) . \quad (43)$$

For the Landau gauge, where $\tilde{Z}_1 = 1$, the STI (42) therefore demands the same feature as non-renormalization. With the decomposition of the vertex (37) this relation demands

$$\lim_{p \rightarrow 0} (A(k^2; q^2, p^2) - B(k^2; q^2, p^2)) = 0 , \quad (44a)$$

$$\lim_{p \rightarrow 0} B(k^2; q^2, p^2) < \infty . \quad (44b)$$

In the infrared limit of the outgoing ghost momentum, $q \rightarrow 0$, the STI (42) yields

$$\Gamma_\mu(p; 0, p) = \Gamma_\mu(-p; 0, -p) , \quad (45)$$

which leads to

$$\lim_{q \rightarrow 0} B(k^2; q^2, p^2) = 0 , \quad (46a)$$

$$\lim_{q \rightarrow 0} A(k^2; q^2, p^2) < \infty , \quad (46b)$$

so that the whole vertex vanishes. Again, the vertex equals the bare vertex in this limit,

$$\Gamma_\mu(p; 0, p) = \Gamma_\mu^{(0)}(0) = 0. \quad (47)$$

In the limit $k \rightarrow 0$ the STI (42) does not provide any further information. There is, however, a hypothesis by Zwanziger which is based on topological arguments [Zwa04]. It states that in the Landau gauge the ghost-gluon vertex remains bare in the infrared limit of any of the legs. Thus, Zwanziger's hypothesis infers in addition to (44), (46):

$$\lim_{k \rightarrow 0} A(k^2; q^2, p^2) = 0, \quad (48a)$$

$$\lim_{k \rightarrow 0} B(k^2; q^2, p^2) < \infty. \quad (48b)$$

Although the identity (42) does not fully constrain the vertex, an ansatz for the ghost-gluon vertex was found in [Sme97] which satisfies (42) and has the correct symmetry properties given by eq. (40):

$$\Gamma_\mu^{(STI)}(k; q, p) = iq_\mu \left(\frac{G(k^2)}{G(q^2)} + \frac{G(k^2)}{G(p^2)} - 1 \right). \quad (49)$$

For an input of this vertex construction, the functions A and B are calculated equivalently to the procedure outlined in section 5.1. It is found that they can be related to their counterparts of the bare vertex input by

$$\begin{aligned} \{A_1, B_1\}|_{\text{STI input}} &= \{A_1, B_1\}|_{\text{bare input}} \left(\frac{G(k^2)}{G(\omega^2)} + \frac{G(k^2)}{G((\omega+k)^2)} - 1 \right) \times \\ &\quad \left(\frac{G((\omega-q)^2)}{G((\omega+k)^2)} + \frac{G((\omega-q)^2)}{G(p^2)} - 1 \right) \end{aligned} \quad (50)$$

$$\{A_2, B_2\}|_{\text{STI input}} = \{A_2, B_2\}|_{\text{bare input}} \left(\frac{G((\omega+k)^2)}{G((\omega-q)^2)} + \frac{G((\omega+k)^2)}{G(p^2)} - 1 \right) \quad (51)$$

Such constructions are promising since they have shown some success, cf. the Ball-Chiu vertex in QED [Bal80]. However, it was shown in [Wat99] that the ansatz (49) is not consistent with perturbation theory. Moreover, it diverges in the infrared limit of the gluon momentum k and thus contradicts Zwanziger's hypothesis (48). This ansatz will be studied in more detail in section 6.2.

6 Results

The results of an explicit calculation of the ghost-gluon vertex according to the preceding section will be performed here both perturbatively and non-perturbatively. The perturbative case can be kept mostly general for a $SU(N_c)$ YM theory in d spacetime dimensions

and a parameter ξ of covariant gauges. On the other hand, the non-perturbative results will be restricted to Landau gauge and either $d = 4$ or $d = 3$. The gauge group will be $SU(3)$, unless indicated.

6.1 Perturbative results

Here, the perturbative ghost-gluon vertex at one-loop order will be calculated. On the one hand, the result may be relevant for studies of perturbative QCD. On the other hand, it lacks the capability of describing the dynamics of YM theory at large distances. However, asymptotic freedom requires the non-perturbative vertex to approach perturbation theory for sufficiently large momenta, and the perturbative calculations therefore provide a check on the non-perturbative vertex in the ultraviolet. In addition, the insights gained from this kind of calculation are of some benefit for the understanding of parts of the underlying mathematical structure. The following calculations are presented for arbitrary Euclidean spacetime dimension d . Any divergent expressions are thus dimensionally regularized [Hoo72]. Eventually, the focus will be on $d = 3$ since the case $d = 4$ is discussed in the literature, see [Wat00, Dav96].

For the implementation of the perturbative calculation, the equation (38) will be employed with the dressing functions of the propagators in the loop, G and Z , set to 1. The scalar integrals $A(k^2; q^2, p^2)$ and $B(k^2; q^2, p^2)$ then become tame enough, albeit vast, to treat them analytically. Using identities for the scalar products such as $\omega \cdot q = \frac{1}{2}(\omega^2 + q^2 - (\omega - q)^2)$ and $\omega \cdot k = \frac{1}{2}(-\omega^2 - k^2 + (\omega + k)^2)$ one can swap back and forth between integrals involving these scalar products directly and the general form of the *triangle integral*,

$$I(\nu_1, \nu_2, \nu_3) \equiv \int \bar{d}^d \omega (\omega^2)^{\nu_1} ((\omega - q)^2)^{\nu_2} ((\omega + k)^2)^{\nu_3}. \quad (52)$$

It is sometimes helpful to visualize that the triangle integral (or equally the vertex) depends on the geometry of a triangle with sides of lengths q , k and p . Integrals of this kind occur in the calculation with both negative and positive values for either of the exponents ν_1, ν_2, ν_3 . We now try to reduce the number of integrals to only a few master integrals with certain values for the exponents.

The first task is to remove the integrals with positive exponents. To do so, one can expand the factor in (52) which has a positive exponent in terms of scalar products and then rewrite the integrals as vector and tensor integrals¹¹. Using the integral identities from

¹¹One can do the calculation more carefully, taking into consideration that there are not only vector integrals with two scales but also some with only one scale and scalar integrals. However, tensor integrals will turn up eventually, and so, since a brute force calculation is necessary, one might as well treat the integrals as all being dependent on two scales.

appendix C one thus finds

$$I(\nu_1, 1, \nu_3) = (q^2 + q \cdot k) I(\nu_1, 0, \nu_3) + \left(1 + \frac{q \cdot k}{k^2}\right) I(\nu_1 + 1, 0, \nu_3) - \frac{q \cdot k}{k^2} I(\nu_1, 0, \nu_3 + 1), \quad (53)$$

$$I(\nu_1, \nu_2, 1) = (k^2 + q \cdot k) I(\nu_1, \nu_2, 0) + \left(1 + \frac{q \cdot k}{q^2}\right) I(\nu_1 + 1, \nu_2, 0) - \frac{q \cdot k}{q^2} I(\nu_1, \nu_2 + 1, 0), \quad (54)$$

$$I(1, \nu_2, \nu_3) = (q^2 - q \cdot p) I(1, \nu_2, \nu_3) + \left(1 - \frac{q \cdot p}{p^2}\right) I(1, \nu_2 + 1, \nu_3) + \frac{q \cdot p}{p^2} I(1, \nu_2, \nu_3 + 1) \quad (55)$$

to decompose the triangle integral where one of the exponents is one and the others are negative. The one-loop calculations also implicate triangle integrals of the kind

$$\begin{aligned} I(\nu_1, 2, \nu_3) &= I(\nu_1, 0, \nu_2) \left(q^4 + 2q \cdot k q^2 - \frac{q^2 k^2 - d(q \cdot k)^2}{d-1} \right) \\ &+ I(\nu_1 + 1, 0, \nu_2) \left(\frac{4(q \cdot k)^2}{k^2} + \frac{2q \cdot k (q^2 + k^2)}{k^2} + 2q^2 + 2 \frac{q^2 k^2 - d(q \cdot k)^2}{(d-1)k^2} \right) \\ &+ I(\nu_1 + 2, 0, \nu_2) \left(1 + 2 \frac{q \cdot k}{k^2} - \frac{q^2 k^2 - d(q \cdot k)^2}{(d-1)k^4} \right) \\ &+ I(\nu_1 + 1, 0, \nu_2 + 1) \left(2 \frac{q^2 k^2 - d(q \cdot k)^2}{(d-1)k^4} - 2 \frac{q \cdot k}{k^2} \right) \\ &+ I(\nu_1, 0, \nu_2 + 1) \left(2 \frac{q^2 k^2 - d(q \cdot k)^2}{(d-1)k^2} - 2 \frac{q \cdot k q^2}{k^2} \right) \\ &+ I(\nu_1, 0, \nu_2 + 2) \frac{q^2 k^2 - d(q \cdot k)^2}{(d-1)k^4}. \end{aligned} \quad (56)$$

Thus, it is possible to remove all positive exponents from within the triangle integrals. In addition, values for the $\{\nu_i\}$ are encountered where one of them is zero turning the triangle integrals into *two-point integrals*. If these incorporate any further positive exponents, the identity

$$I(0, 1, \nu) = I(0, 0, \nu + 1) + (q - k)^2 I(0, 0, \nu) \quad (57)$$

can be applied to finally end up with integrals with negative exponents only. Using the method of integration by parts, see [Tka81, Che81], one can now manipulate the triangle and two-point integrals such that exponents with $\nu_i < -1$ can be increased, cf. [Wat00]. At the end of the day one is left with only four integrals, namely $I(1, 1, 1) =: \Phi^{(d)}(k; q, p)$, $I(1, 0, 1) =: \Xi^{(d)}(k)$, $I(1, 1, 0) \equiv \Xi^{(d)}(q)$ and $I(0, 1, 1) \equiv \Xi^{(d)}(p)$.

From eq. (57) one can anticipate that some apparently divergent integrals of the kind $\int \vec{d}^d \omega / \omega^2$, $\int \vec{d}^d \omega / (\omega - q)^2$ and $\int \vec{d}^d \omega / (\omega + k)^2$ will occur. Allowing shifts of the integration variable, these contributions mutually cancel in each graph separately for any gauge parameter. However, the integral $\int \vec{d}^d \omega / \omega^4$ remains. It is originated in the part of the gluon propagator that is proportional to its momentum vector. Consequently, this integral vanishes only in the Feynman gauge ($\xi = 1$). We omit this term referring to [Col84], ch. 4, where it is stated that integrals of this type actually are zero in the framework of dimensional regularization.

The procedure of manipulating the various integrals can now be applied to the perturbative version of (38) to obtain the one-loop ghost-gluon vertex in arbitrary dimension and covariant gauge. The calculation is straightforward but tedious and only the lengthy results are stated here:¹²

$$\begin{aligned}
A(k^2; q^2, p^2) &= \frac{g_d^2 N_c}{64\Delta} \left\{ \frac{1}{2} \Phi^{(d)}(k; q, p) \left[-(p^2 - q^2)^2 (p^2 + q^2) (d^2(\xi - 1)^2 + 8\xi(2\xi - 3) - \right. \right. \\
&\quad 2d(3 - 7\xi + 4\xi^2)) - k^6(4 + d^2(\xi - 1)^2 - 8\xi + 12\xi^2 - 2d(1 - 5\xi + 4\xi^2)) + \\
&\quad k^4(p^2(d^2(\xi - 1)^2 - 8 + 32\xi - 2d(-3 + \xi + 2\xi^2)) + q^2(d^2(\xi - 1)^2 + 6d(1 + \xi - 2\xi^2) + \\
&\quad 8(\xi - 1 + 3\xi^2))) + k^2(q^4(d^2(\xi - 1)^2 + 4(3 - 10\xi + \xi^2) - 2d(7 - 9\xi + 2\xi^2)) - \\
&\quad 2p^2q^2(20 + d^2(\xi - 1)^2 - 28\xi - 2d(5 - 7\xi + 2\xi^2)) + p^4(d^2(\xi - 1)^2 - \\
&\quad \left. \left. 2d(7 - 13\xi + 6\xi^2) + 4(3 - 16\xi + 7\xi^2)) \right) \right] + \\
&\Xi^{(d)}(q) \left[k^4(\xi - 1)(d(5 - 9\xi) - 6 + d^2(\xi - 1) + 16\xi) - 2k^2(-q^2(8 + 3d(\xi - 1) - \right. \\
&\quad 10\xi)(1 + \xi) + p^2(\xi - 1)(d(4 - 8\xi) - 2 + d^2(\xi - 1) + 14\xi)) + (p^2 - q^2)(p^2(\xi - 1) \times \\
&\quad (2 + d(3 - 7\xi) + d^2(\xi - 1) + 12\xi) + d^2(\xi - 1) + 12\xi) + q^2(6 - 7d(\xi - 1)^2 + \\
&\quad \left. d^2(\xi - 1)^2 - 26\xi + 12\xi^2) \right] + \\
&\Xi^{(d)}(k) \left[-k^4(d(8 - 6\xi) + 4(\xi - 5) + d^2(\xi - 1))(\xi - 1) + (p^2 - q^2)^2(d^2(\xi - 1)^2 + \right. \\
&\quad 8\xi(2\xi - 3) - 2d(3 - 7\xi + 4\xi^2)) + 2k^2(q^2(2 + d + 2\xi^2 - d\xi^2) + \\
&\quad \left. p^2(2 + d + 12\xi - 4d\xi - 10\xi^2 + 3d\xi^2)) \right] + \\
&\Xi^{(d)}(p) \left[k^4(6 - 5d(\xi - 1)^2 + d^2(\xi - 1)^2 - 14\xi + 4\xi^2) - 2k^2((-8 + 3d)p^2(\xi - 1)^2 + \right. \\
&\quad q^2(2 + d^2(\xi - 1)^2 - 14\xi + 14\xi + 8\xi^2 - 2d(2 - 5\xi + 3\xi^2))) - (p^2 - q^2)(p^2(6 - \\
&\quad 7d(\xi - 1)^2 + d^2(\xi - 1)^2 - 22\xi + 12\xi^2) + q^2(d^2(\xi - 1)^2 + \\
&\quad \left. d(-3 + 10\xi - 7\xi^2) + 2(-1 - 7\xi + 6\xi^2)) \right] \} \tag{58a}
\end{aligned}$$

¹²Note that all angles have been eliminated in favor of the absolute values of q , k and p .

$$\begin{aligned}
B(k^2; q^2, p^2) &= \frac{g_d^2 N_c}{128 \Delta k^2} \left\{ \frac{1}{2} \Phi^{(d)}(k; q, p) \left[(2-d)k^8(2+d(\xi-1)-6\xi)(\xi-1) + \right. \right. \\
&\quad (d-4)(p^2-q^2)^3(p^2+q^2)(d(\xi-1)-4\xi)(\xi-1) + 2k^6(\xi-1)(-2(d-3)q^2(1+\xi) + \\
&\quad p^2(-2+d(2-6\xi)+d^2(\xi-1)+6\xi)) - 2k^2(p^2-q^2)(p^4(\xi-1)(-2+d(6-10\xi) + \\
&\quad d^2(\xi-1)+22\xi) + 2(d-3)q^4(\xi^2-1) - p^2q^2(16+d^2(\xi-1)^2 - 32\xi - 4d(3-4\xi + \\
&\quad \xi^2))) - 2k^4(2p^4(1+2d(\xi-1)-7\xi)(\xi-1) - q^4(\xi-1)(-2+d(4-8\xi) + \\
&\quad d^2(\xi-1)+14\xi) + p^2q^2(d^2(\xi-1)^2 - 4d(3-5\xi+2\xi^2) + 4(7-14\xi+3\xi^2))) \left. \right] + \\
&\quad \Xi^{(d)}(q) \left[(3-d)(p^2-q^2)^2(p^2+q^2)(d(\xi-1)-4\xi)(\xi-1) + k^6(\xi-1)(d(5-9\xi) - 4 + \right. \\
&\quad d^2(\xi-1)+16\xi) + k^2(p^4(\xi-1)(-4+d(11-23\xi)+3d^2(\xi-1) + \\
&\quad 40\xi) - q^4(4+d^2(\xi-1)^2 - 52\xi+32\xi^2+d(-9+22\xi-13\xi^2)) - 2p^2q^2(d^2(\xi-1)^2 + \\
&\quad d(-9+14\xi-5\xi^2)+4(2-5\xi+\xi^2))) + k^4(-p^2(\xi-1)(-8+d(13-25\xi) + \\
&\quad 3d^2(\xi-1)+44\xi) + q^2(d^2(\xi-1)^2 - 3d(5-6\xi+\xi^2) - 4(-8+11\xi+\xi^2))) \left. \right] + \\
&\quad \Xi^{(d)}(k) \left[(4-d)(p^2-q^2)^3(d(\xi-1)-4\xi)(\xi-1) - k^6(d^2(\xi-1)^2 + 4(6-9\xi+\xi^2) - \right. \\
&\quad 2d(5-8\xi+3\xi^2)) + k^4(-q^2(-8-4d(-2+\xi)+d^2(\xi-1))(\xi-1) + p^2(12d(\xi-1) + \\
&\quad d^2(\xi-1)^2 - 16(-2+2\xi+\xi^2))) + k^2(p^2-q^2)(-q^2(d^2(\xi-1)^2 + 4\xi(-7+5\xi) - \\
&\quad 2d(3-8\xi+5\xi^2)) + p^2(d^2(\xi-1)^2 - 2d(1-8\xi+7\xi^2) + 4(-2-5\xi+9\xi^2))) \left. \right] + \\
&\quad \Xi^{(d)}(p) \left[(d-3)(p^2-q^2)^2(p^2+q^2)(d(\xi-1)-4\xi)(\xi-1) + k^6(4(1-4\xi+\xi^2) + \right. \\
&\quad d^2(\xi-1)^2 - 5d(\xi-1)^2) - k^4(p^2(d^2(\xi-1)^2 + 4(\xi-2-3\xi^2) + d(2\xi-3+\xi^2)) + \\
&\quad q^2(d^2(\xi-1)^2 + d(10\xi-3-7\xi^2) + 4(3\xi^2-2-5\xi))) - k^2(q^4(4(3-2\xi+\xi^2) + \\
&\quad d^2(\xi-1)^2 - 5d(\xi-1)^2) - 2p^2q^2(d^2(\xi-1)^2 + d(22\xi-9\xi^2-13) + 4(5-11\xi + \\
&\quad 4\xi^2)) + p^4(d^2(\xi-1)^2 + d(-5+18\xi-13\xi^2) + 4(3-8\xi+7\xi^2))) \left. \right] \right\} . \quad (58b)
\end{aligned}$$

In the 3-dimensional case the scalar integrals yield the following results (see appendix C):

$$\Phi^{(3)}(k, q, p) = \frac{1}{8\sqrt{q^2 k^2 p^2}}, \quad (59)$$

$$\Xi^{(3)}(q) = \frac{1}{8\sqrt{q^2}}. \quad (60)$$

In the Landau gauge, the expression A and B then shrink from (58) down to

$$A(k^2; q^2, p^2) \Big|_{\substack{\xi=0 \\ d=3}} = \frac{g_3^2 N_c}{2} \frac{7k^3 - 5k(p-q)^2 + 7k^2(p+q) - 9(p-q)^2(p+q)}{128k^3pq(k+p+q)}, \quad (61a)$$

$$\begin{aligned}
B(k^2; q^2, p^2) \Big|_{\substack{\xi=0 \\ d=3}} &= \frac{g_3^2 N_c}{2} \frac{1}{256k^3pq(k+p+q)} (k^5 + 5k^4(p+q) + 3k(p-q)^3(p+q) + \\
&\quad 3(p-q)^3(p+q)^2 - 2k^2(p-q)(4p^2 + 9pq - 3q^2) + k^3(6q^2 + 14pq - 4p^2)) . \quad (61b)
\end{aligned}$$

A simple choice of the momentum configuration is given by choosing all momenta to be of the same magnitude. One obtains

$$A(p^2, p^2, p^2)|_{d=3} = \frac{g_3^2 N_c}{2} \frac{21 + 12\xi - \xi^2}{384} \frac{1}{p}, \quad (62a)$$

$$B(p^2, p^2, p^2)|_{d=3} = \frac{g_3^2 N_c}{2} \frac{27 + 6\xi - \xi^2}{768} \frac{1}{p}. \quad (62b)$$

Evidently, in the ultraviolet momentum regime the one-loop contributions vanish on account of asymptotic freedom.

In order to check the result for any dimension, one can inspect the implications of the Slavnov-Taylor identity for the ghost-gluon vertex as discussed in section 5.3. In the infrared limit of the incoming ghost momentum p the result (58) yields

$$\lim_{p \rightarrow 0} (A(k^2; q^2, p^2) - B(k^2; q^2, p^2)) = \frac{1}{4} g_a^2 N_c \xi \Xi^{(d)}(q), \quad (63)$$

and thus fulfills the first condition given by eq. (44a) for $\xi = 0$. The second condition (44b) requires the function B to be finite in this limit. For $d = 4$ the two-point integrals have a simple pole (see appendix C) and therefore it is not trivial to show the finiteness of B in this case. For dimensions d , however, in which the two-point integrals are finite, we find

$$\lim_{p \rightarrow 0} B(k^2; q^2, p^2) \sim \lim_{p \rightarrow 0} (C_1 \Xi(p) + C_2 q^2 \Phi(k, q, p)), \quad (64)$$

where the coefficients C_1 and C_2 yield $(C_1 + C_2) \sim \xi$. For $d = 3$, the integrals involved in (64) can be related by $\Xi(p) = q^2 \Phi(-q, q, p)$. Hence, the function B stays finite in the limit $p \rightarrow 0$ for $\xi = 0$ in this case. Thus, it was explicitly shown that for $d = 3$ the perturbative one-loop ghost-gluon vertex reduces to the bare vertex as the incoming ghost momentum goes to zero if and only if the gauge parameter is chosen to be $\xi = 0$ (Landau gauge).

Further investigations of the case $d = 3$ show that the implication (46) for the infrared limit of the outgoing ghost momentum q is fulfilled for any gauge parameter ξ . In the limit $k \rightarrow 0$, the perturbative vertex suffices (48) and thus reduces the vertex to its tree-level value in this limit. The latter result is also found for $d = 3$ and any gauge parameter ξ .

For any spacetime dimension other than $d = 3$, the validity of some of the implications of the vertex's STI are found to be restricted to the choice $\xi = 1$ (Feynman gauge)¹³. Since the Feynman gauge is also the only choice for which the $\int \bar{d}^d \omega / \omega^4$ terms mutually cancel, it seems possible that the violation of the STI for $\xi \neq 1$ is due to the fact that the $\int \bar{d}^d \omega / \omega^4$ terms were erased by hand (see above). A closer focus on $d \neq 3$ therefore requires a check if the integration by parts method produces additional surface terms or if the neglect of $\int \bar{d}^d \omega / \omega^4$ terms is justified as stated in [Col84].

¹³The terms which do not satisfy the STI's implication are proportional to $(d-3)(\xi-1)$.

Whereas it was shown for $d = 3$ that the perturbative vertex reduces to the bare vertex in the infrared limit of any one of the momenta, the object $(A - B)$ diverges if *all* momenta are taken to zero, also for the Landau gauge,

$$\lim_{p \rightarrow 0} (A(p^2, p^2, p^2) - B(p^2, p^2, p^2)) \Big|_{d=3} = \lim_{p \rightarrow 0} \frac{g_3^2 N_c}{2} \frac{15 + 18\xi - \xi^2}{768p}. \quad (65)$$

Compared to eq. (63), this indicates that the functions A and B have non-interchangeable infrared limits. This issue will be addressed again in the next section. Nonetheless, eq. (65) represents an infrared singularity of perturbation theory. It is with great anticipation to find out whether or not this singularity persists for the non-perturbative vertex. An infrared singular non-perturbative ghost-gluon vertex could be fatal for the assumptions made for the propagators.

6.2 Non-perturbative results

The following computation of the ghost-gluon vertex in the Landau gauge with non-perturbative propagators employs the Dyson-Schwinger equation (36) in such a way that the bare ghost-gluon vertex is used as a starting point of an iteration. The exact non-perturbative ghost-gluon vertex (leaving aside the truncation of four-point functions) would require a full iteration to self-consistency, a highly complicated task since the propagators would have to be calculated simultaneously. A reasonable approach is therefore to do only one iteration step. Zwanziger's hypothesis and non-renormalization indicates that the bare vertex is quite close to the fixed point of the iteration. The outcome of the calculation will tell us more about the validity of this statement.

The numerical integration of the loop momenta has been carried out using exponentially stretched Gauss-Legendre quadrature [Pre92], taking into account the pole structure of the integrand. For more details on dealing with triangle integrals analytically and numerically, see appendix C.4. The perturbative results for $d = 3$ given in section 6.1 have been checked and verified numerically. Some minor deviations occurred in the infrared behavior apart from the limits concerned with the STI. These might be understood to be due to the neglect of the integrals of the form $\int \bar{d}^d \omega / \omega^4$ in the analytical calculations.

Throughout, the results will be displayed for three- and four-dimensional spacetime, in order to directly point out the differences and similarities. For the practical implementation of the calculation one has to bear in mind some subtle differences between four and three dimensions. First of all, the gauge coupling in three dimensions, g_3 , has a mass dimension of $1/2$ whereas in four dimensions it is just a number. This can be seen directly from the dimensionless action where the kinetic parts determine the dimension of the fields and as a consequence the coupling terms lead to [Mut98]

$$[g_d] = [\text{mass}]^{(2-\frac{d}{2})}. \quad (66)$$

Secondly, one is not to forget the dimension dependence of the phase space factor $(2\pi)^{-d}$ in the integrals and contractions of the kind $g_{\mu\nu}g^{\mu\nu} = d$. For the integration in d -dimensional spherical coordinates, the details given in [Vel94] will be helpful. The dressing functions of the propagators for four and three dimensions are to be distinguished as shown in section 4.

The strongest implication from first principle on the vertex to be checked is the reduction to the bare vertex in the infrared limit of the incoming ghost momentum p . The technical issue of taking infrared limits numerically is outlined in appendix E. According to (44), the vanishing of $(A - B)$ and a finite function B yields a bare vertex in the limit $p \rightarrow 0$. In addition, the STI implies that for a vanishing outgoing ghost momentum q , the whole vertex is supposed to vanish in the manner given by (46). In figure 5 it can be seen that this turns out to be well-fulfilled both in four and three dimensions. It is worth pointing out that *both* graphs in fig. 2 which contribute to the vertex apart from the bare vertex comply with the implications of the STI separately.

With both implications from the STI fulfilled, it can be concluded that gauge invariance of physical quantities is not (additionally) broken in the infrared limit by this particular choice of the vertex. Although the results have been somewhat expected with non-renormalization of the vertex in mind, the verification of the STI's implications are crucial for the validity of this construction of the vertex.

We now turn our attention to the infrared limit of the gluon momentum where one cannot rely on statements from first principle. The behavior found is shown in fig. 6. Both in four and three dimensions the vertex reduces almost to its tree-level form. According to (48), the function B stays finite, whereas $A(0; p^2, p^2)$ stays small relative to the tree-level value. In the ultraviolet of the momentum p^2 , the function $A(0; p^2, p^2)$ approaches the tree-level value due to asymptotic freedom, in the infrared it shows a small undershoot of about 10% – 15%.

The deviation of the vertex from the tree-level value found in the limit $k \rightarrow 0$ is small enough to argue that it might be an artifact of the truncation on the one hand, and on the other hand it is likely to decrease after further iteration steps. Zwanziger's hypothesis of a bare ghost-gluon vertex in the infrared is thus approximately fulfilled. The above results therefore strengthens the evidence for the Zwanziger-Gribov scenario with infrared ghost dominance in the Landau gauge.

The qualitative behavior for intermediate and ultraviolet momenta has shown to be similar for all momentum configurations. To investigate this further, let us consider the vertex for all three momenta of the same magnitude, i.e. the kinetic point $(p^2; p^2, p^2)$. The transverse projection of the non-perturbative vertex (39) compared to the perturbative one is plotted in fig. 7. For four as well as for three dimensions, the vertex is found to not deviate far from the bare vertex for the whole range of momenta. Deviations are in the range of 15%.

The results for three dimensions show, starting from about $10g_3^2$, a perturbative behavior which is mirrored in the fact that the propagators also become perturbative in this mo-

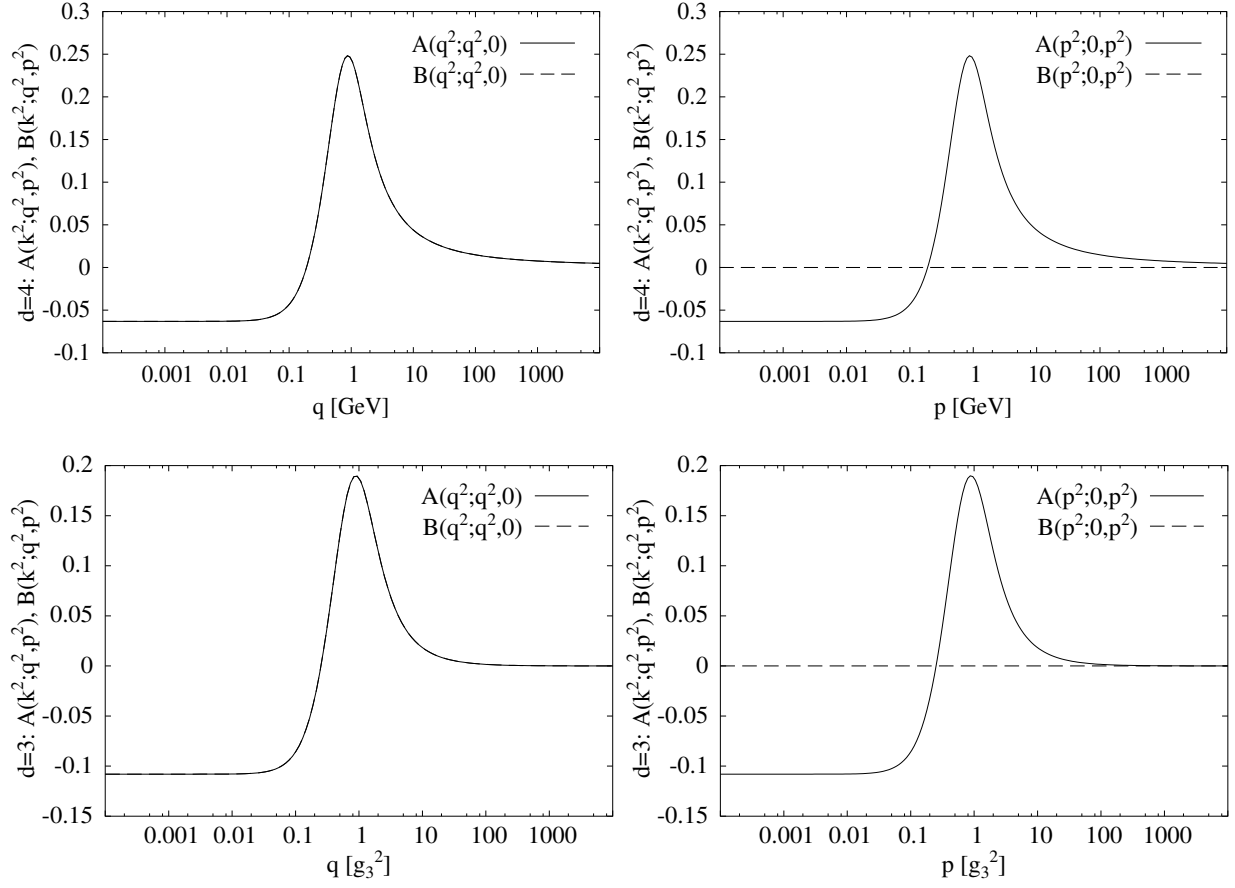


Figure 5: The infrared limit for the ghost momenta of the vertex in four dimensions (upper plots) and three dimensions (lower plots). Evidently (left panel), $A(q^2; q^2, 0) = B(q^2; q^2, 0)$ for all $q \equiv -k$. For $q \rightarrow 0$ (right panel), $B(p^2; 0, p^2) = 0$ and $A(p^2; 0, p^2) < \infty \forall p \equiv k$ is observed.

6 RESULTS

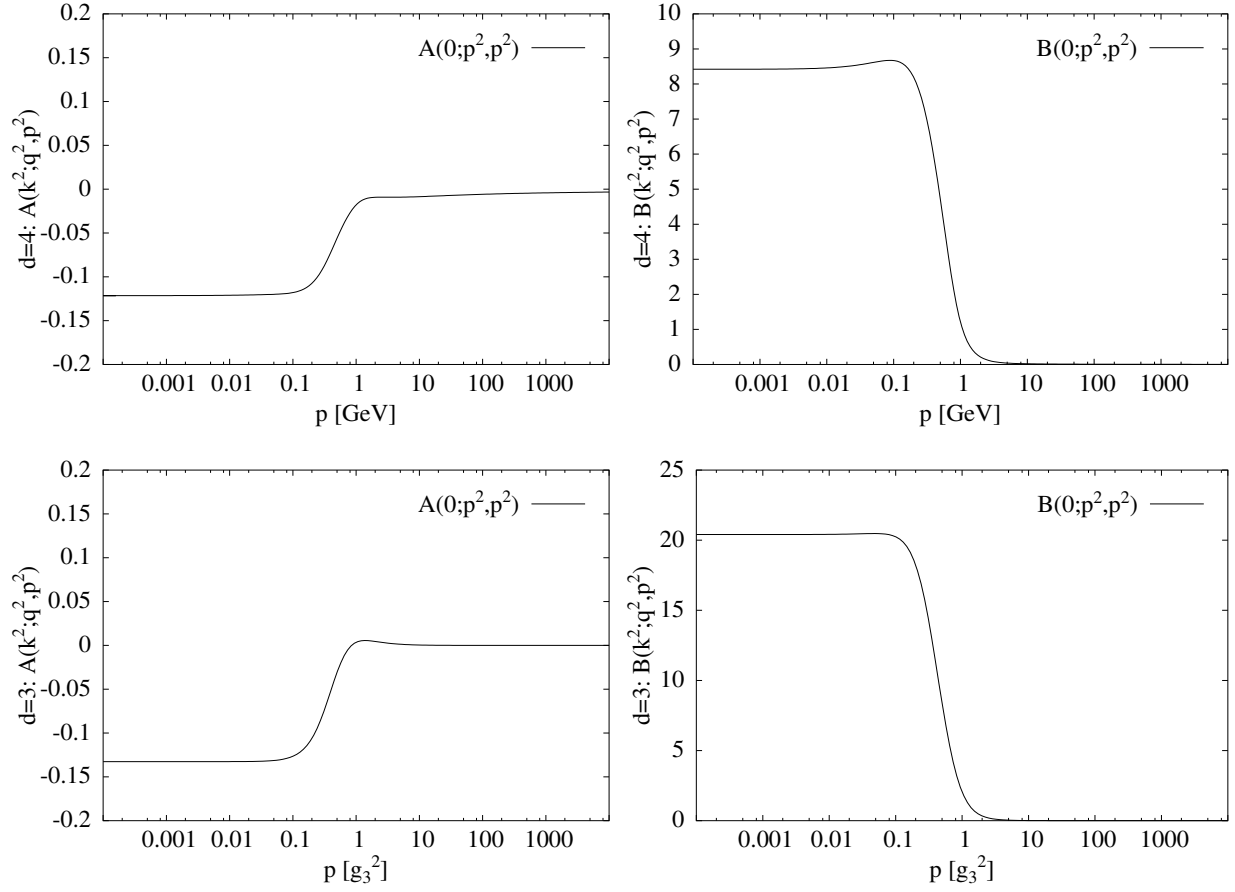


Figure 6: The infrared limit $k \rightarrow 0$ of the vertex. The upper plots are for $d = 4$ and the lower ones for $d = 3$.

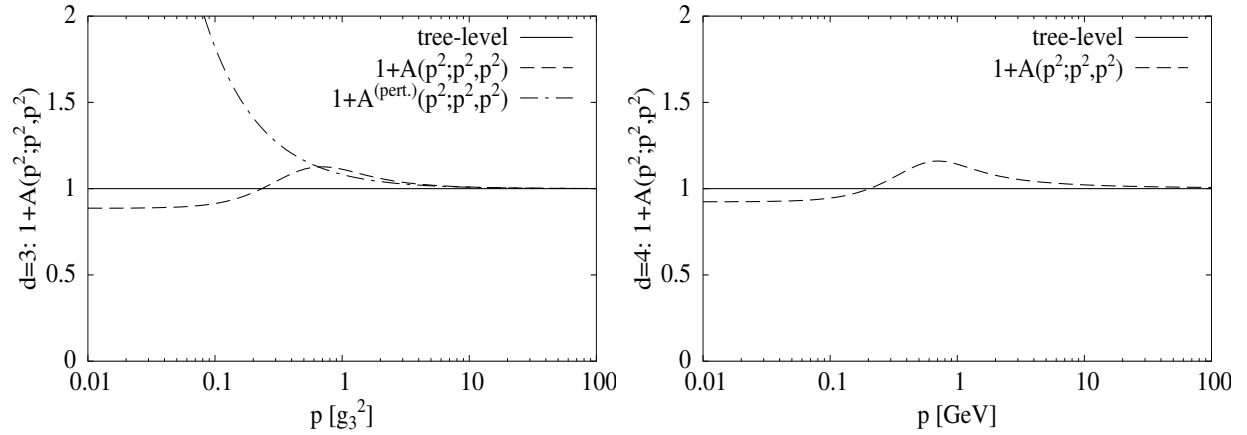


Figure 7: $d = 3$ (left) and $d = 4$ (right) vertex for momenta equal in magnitude. Perturbative behavior and reduction to bare vertex in the UV are shown.

mentum regime (see figs. 3 and 4). Because for $d = 3$ the gauge coupling constant has a mass dimension of $1/2$, a perturbation series of a Green function must always involve terms with powers of g_3^2/p with some momentum p , instead of just g_3^2 . Other scales with a mass dimension are not available in the finite three-dimensional YM theory. In the ultraviolet, the resummed perturbative Green function therefore is well-approximated by leading-order perturbation theory. Asymptotic freedom for $d = 3$ is thus articulated in the reduction of the non-perturbative vertex to the one-loop perturbative vertex.

In four dimensions, the non-perturbative vertex fails to equal leading-order perturbation theory. The dimensionless gauge coupling g_4 does not guarantee that the first terms of an expansion in g_4 are leading in the ultraviolet, as for $d = 3$. A resummation would be necessary to find a perturbative vertex asymptotic to the non-perturbative one. The perturbative one-loop vertex actually yields all but a constant for the kinetic point $(p^2; p^2, p^2)$ and is therefore not displayed in figure 7. This can be understood from dimensional arguments. Since there is no parameter with a mass dimension in $d = 4$ perturbation theory, due to the non-renormalization of the vertex, and the function A is to be dimensionless, it can only depend on ratios of the momenta. Therefore, at a kinetic point where all momenta are the same, A produces a constant.

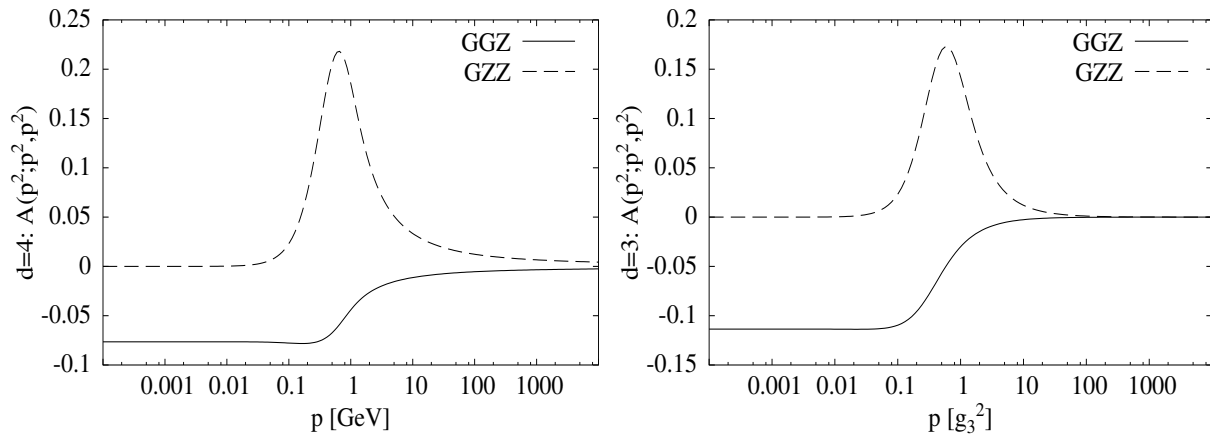


Figure 8: Separate contributions to the vertex for $d = 4$ (left) and $d = 3$ (right). GGZ is the contribution to A from the graph with two ghost- and one gluon propagator, GZZ accounts for the graph with one ghost- and two gluon propagators (see fig. 2).

The characteristic bump found for the intermediate momentum regime is reminiscent of the bump in the gluon propagator, see figs. 3 and 4. The origin of the bump in fig. 7 is actually found in the graph that contributes with two gluon propagators inside the loop, see fig. 8, so that we are led to the conclusion that the behavior of the gluon propagator presumably dictates the behavior of the vertex for intermediate momenta. The contributions from the two different graphs to the function A shown in fig. 8 also provide an explanation for the sign change at intermediate momenta. It is shown that the graph with two ghost propagators is the leading contribution in the infrared with a negative sign. In the sum of the two

graphs the function A will therefore undergo a sign change. The infrared dominance of the graph with the two ghost propagators in the loop indicates that the infrared behavior of the vertex be dictated by ghosts.

Since the vertex depends on three independent scales, one can hardly display all momentum configurations. A generalization of the specific choices considered above is given by the kinematic points $(p^2; ap^2, p^2)$ and $(p^2; p^2, ap^2)$ where momentum conservation constrains $a \in [0, 4]$. Varying a , the behavior of the functions A and B is shown in fig. 9. At this point it is worth while to look at the symmetry properties of the vertex. The function $A(p^2; p^2, ap^2)$ yields the exact same behavior as $A(p^2; ap^2, p^2)$ shown in fig. 9 for all parameters a . The value of the gluon momentum does not alter this behavior. The inspections of the STI in figure 5 provide supplementary results. Hence, the symmetry property (40) is fulfilled. For the function B , on the other hand, a (anti)symmetry is neither expected nor found (see sec. 5.2). The combination $B - (1 + A)/2$ does not show any antisymmetry either, as predicted for gauges that are not manifestly ghost-antighost symmetric. The symmetry properties will not be altered by the quantitative behavior of the propagators, the distinction between four and three dimensions is therefore redundant. Nevertheless, the three-dimensional results are depicted here as well for completeness.

The plots in fig. 9 most effectively expose one of the features of the vertex functions A and B : the infrared limits of these functions seem to be non-uniform. Depending on the geometry of the triangle formed by the three momenta, A (or B) will approach different values for all momenta at zero. This behavior was already found for the perturbative vertex, see page 28. The entire non-perturbative vertex, on the other hand, multiplying the functions A and B with q_μ and k_μ , resp., has an unambiguous infrared limit. For a further discussion on this issue, see appendix E.

The running coupling in four dimensions as it was investigated in [Sme98b] can now undergo a correction by the ghost-gluon vertex. The renormalization constant of the vertex, \tilde{Z}_1 , had been defined in the infrared limit of the incoming ghost momentum to exploit non-renormalization and obtain $\tilde{Z}_1 = 1$, see eq. (29). Now we can redefine the renormalization constant by $\tilde{Z}_1(p^2) = 1 + A(0; p^2, p^2)$ [Cuc04] and find a running coupling $\alpha = g_4^2/(4\pi)$ with vertex correction [Mut98]

$$\alpha(p^2) = \tilde{Z}_1^2(p^2)G^2(p^2)Z(p^2). \quad (67)$$

The result is depicted in fig. 10 and shows that this definition enforces a bump in the running coupling¹⁴, a behavior which seems peculiar for the renormalization group because the β function acquires a non-trivial zero [Alk03]. However, this may be due to the truncation since intermediate momenta are the least trustworthy regime of the truncation scheme. It is still under debate to which extent this is a problematic feature of the solutions.

¹⁴This behavior is similar to the results for the propagators shown in sec. 4.

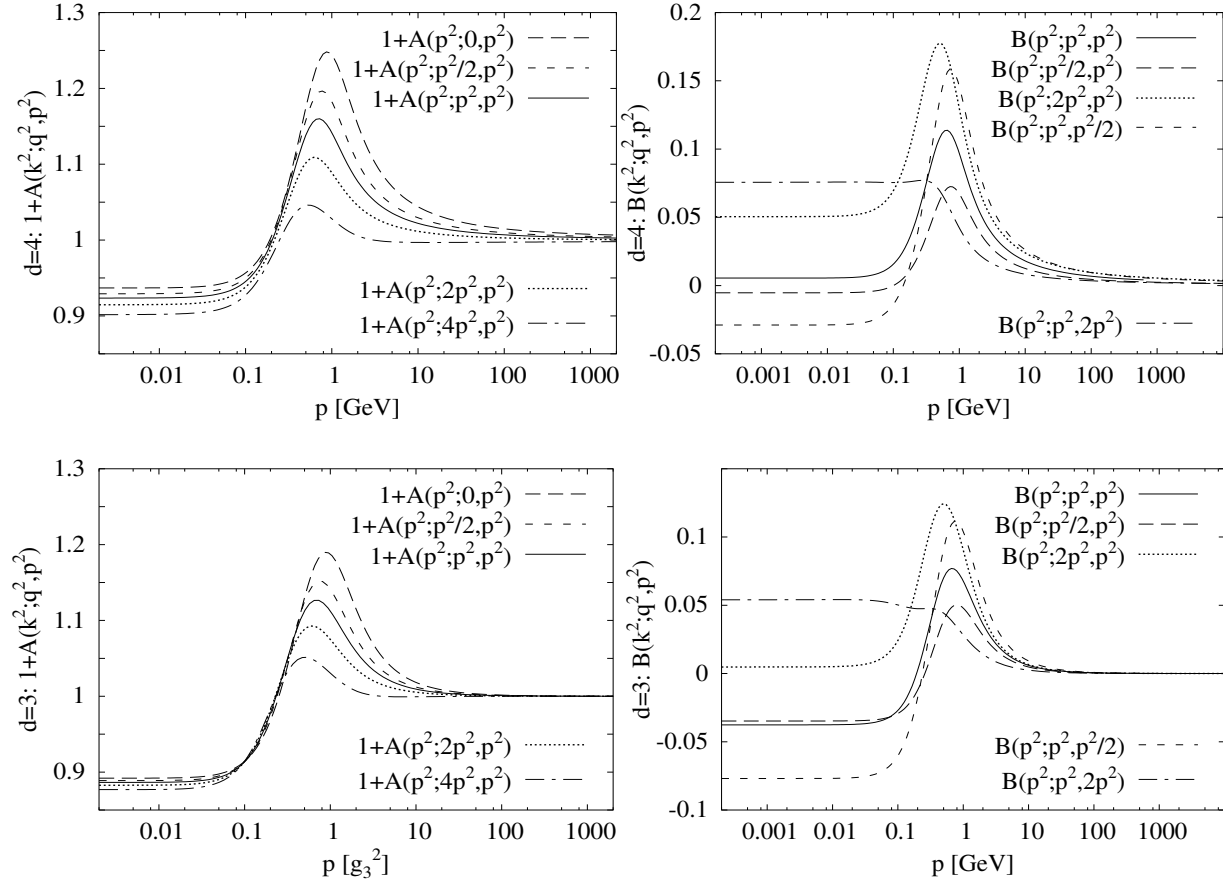


Figure 9: Non-symmetric momentum configurations of the 4d vertex (upper plots) and the 3d vertex (lower plots). It is found that $A(p^2; ap^2, p^2) = A(p^2; p^2, ap^2)$ (left panel). The function B (right panel) does not show any symmetry properties, i.e. $B(k^2; aq^2, p^2) \neq \pm B(k^2; q^2, ap^2)$.

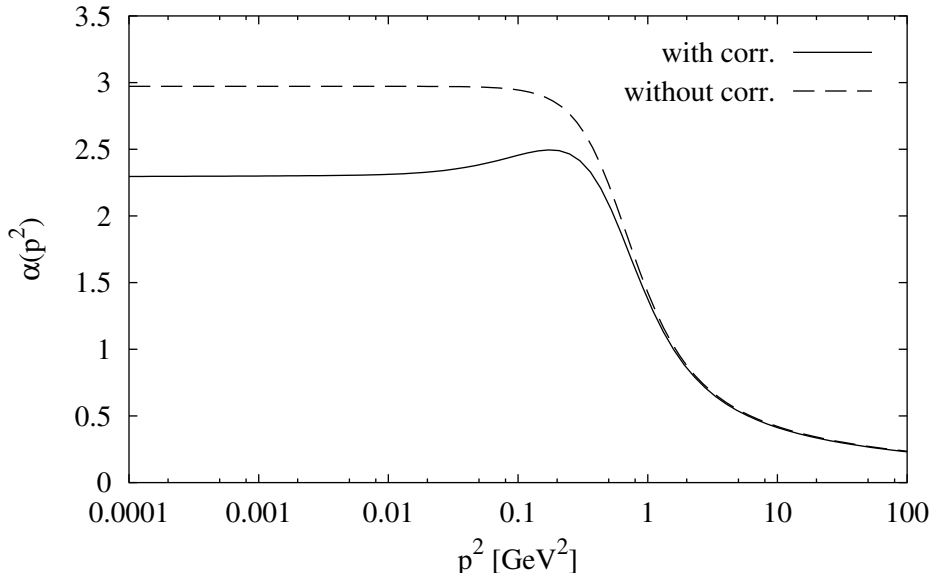


Figure 10: Vertex correction to the running coupling given in ref. [Fis02]. The result for α without vertex correction is a fit which eliminates the bump that usually occurs.

STI-motivated vertices

Previous studies [Ler02] considered constructions of the ghost-gluon vertex motivated by the corresponding STI [Sme98b], such as the one given by eq. (49). The assessment of this construction required an insertion of the vertex into the DSEs for the propagators, finding the propagators do not react sensitively to the altered vertex input. By means of the computational mechanism developed here it is now feasible to investigate further the STI-motivated ansatz for the ghost-gluon vertex. Instead of the bare vertex, the construction (49) has been used as an input into the DSE for the ghost-gluon vertex. The three-gluon vertex is used at tree-level, as before. The results show, see fig. 11, that one iteration step leads to a function A of the vertex that is qualitatively as well as quantitatively more similar to the bare vertex than it is to the input, i.e. the STI-motivated vertex. The deviation of the function B from zero can be ignored since in the Landau gauge these contributions will be eliminated when contracted with transverse gluon propagators.

With the calculation understood in terms of an iteration, one can estimate the bare vertex to be closer to the fixed point than the STI-motivated vertex is. This indicates that the bare ghost-gluon vertex is a better choice for DSE studies than the construction from the STI given by (49). Moreover, the infrared behavior of the STI-motivated vertex does not comply with Zwanziger's hypothesis since it is singular for zero gluon momentum. The STI for the vertex does apparently not provide enough information for constructing the

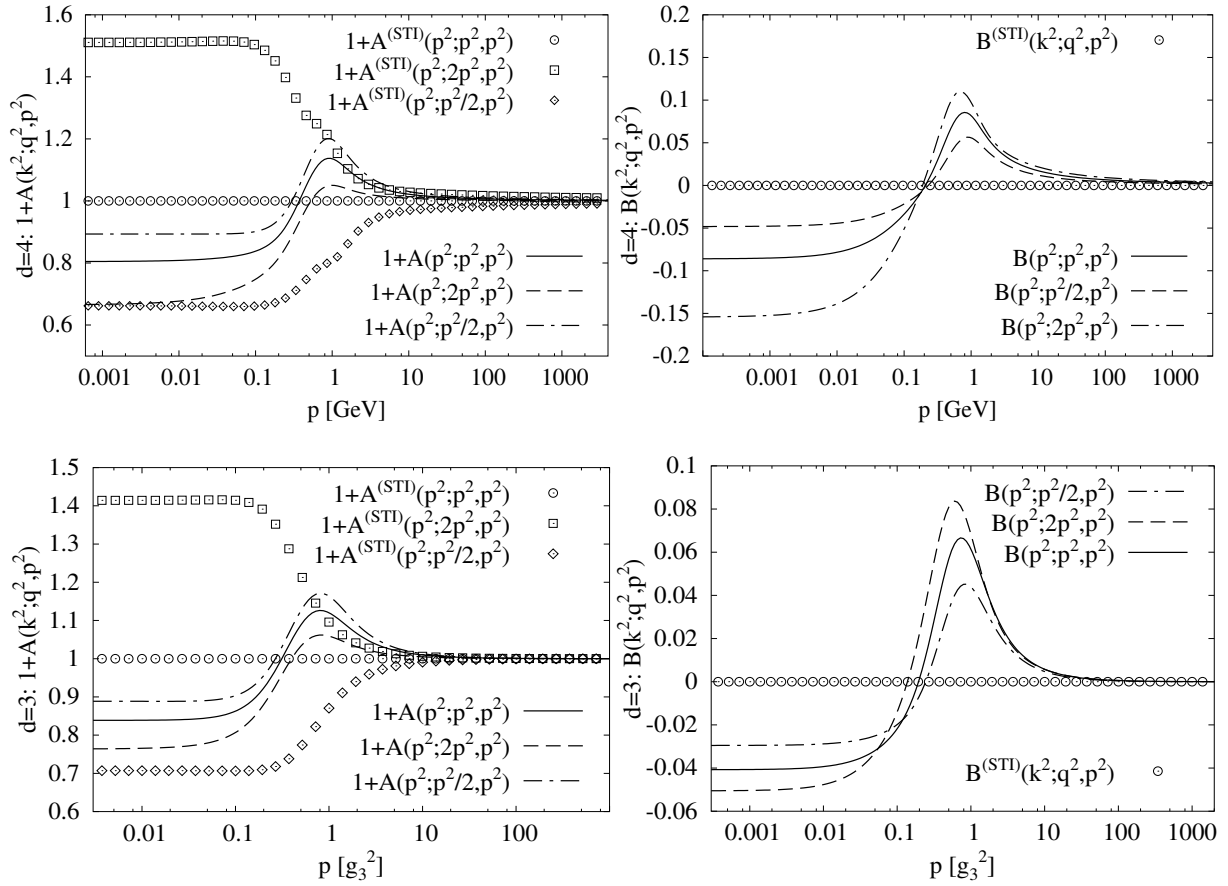


Figure 11: By comparison, the input and output of the STI-motivated ghost-gluon vertex. The function A (left) and the function B (right) are shown on the upper row for $d = 4$, and for $d = 3$ on the lower row.

vertex from it.

Another vertex ansatz developed and discussed in [Sme98b, Ler02] which is motivated by the STI of the vertex,

$$\Gamma_\mu(k; q, p) = iq_\mu \frac{G(k^2)}{G(q^2)}, \quad (68)$$

but does not satisfy the symmetry property (40) was investigated as well. Qualitatively, it showed the same reduction to a vertex close to tree-level as the other STI-motivated vertex discussed above.

Generally speaking, the DSE of the ghost-gluon vertex has turned out to be quite insensitive to the input of the ghost-gluon vertex into its right hand side. The propagators, on the other hand, are the objects which determine the behavior of the vertex most influentially. An investigation has been done varying the fit parameters of the propagators slightly to observe the influence on the vertex. The outcome was that the quantitative behavior is dictated by the changes of the propagators. As above, the ghost propagator dominates the infrared, whereas the gluon propagator determines the intermediate momentum regime.

Comparison to lattice data

Recently, lattice calculations on the Landau gauge ghost-gluon vertex for $d = 4$ have become available [Cuc04]. The $SU(2)$ results obtained there are for the kinematic points $(0; p^2, p^2)$, i.e. the infrared limit of the gluon leg which is not known from first principles. The results are, as can be seen in fig. 12, in good agreement with the $SU(2)$ results from DSE studies presented here¹⁵. It seems that for a symmetric lattice direction¹⁶ the data comply better with our results than for the asymmetric direction. In the infrared limit of all momenta, the lattice calculation is limited due the finite lattice size. The smallest momentum p available on the lattice is 366 MeV , and this only at the expense of an asymmetrical lattice direction. Therefore, the behavior for $p \rightarrow 0$ with the undershoot still remains a crucial prediction of the DSE calculations. The agreement with lattice data is a confirmation of the calculations performed here. It indicates that the truncation induced breaking of gauge invariance is under good control. Lattice theory does not involve any truncation artifacts as for DSE studies and it also does not suffer from any such formal weak points as the mathematically rigorous definition of the path integral formalism. Nevertheless, for the lattice theory the question is only deferred to other problems, such as whether or not the continuum limit can be defined rigorously.

¹⁵By assumption, the coupling g_4 has been used as for $SU(3)$, but N_c has been set to 2.

¹⁶Symmetric and asymmetric directions on the lattice are distinguished to account for the systematic errors due to the breaking of rotational symmetry.

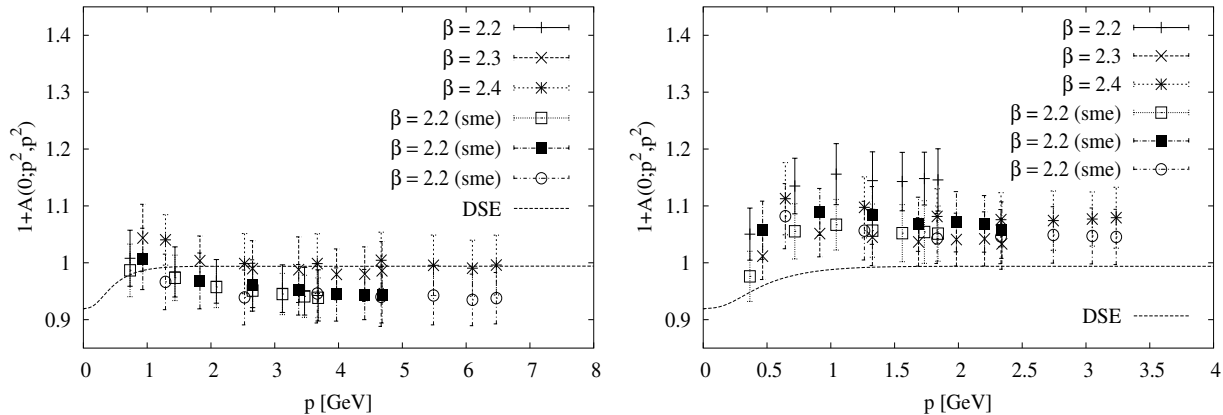


Figure 12: Comparison of the DSE results to recent lattice data [Cuc04]. On the left panel, the lattice data were obtained with a symmetric lattice direction, one the right panel with an asymmetric one.

7 Conclusions

The non-perturbative ghost-gluon vertex has been approximately calculated. For this purpose, its Dyson-Schwinger equation has been derived and a solution to it has been pursued by means of an iteration employing non-perturbative propagators. A specific feature of the Landau gauge, the non-renormalization of the vertex, has motivated to choose the bare vertex as a starting point. Performing one iteration step has resulted in a vertex which qualitatively as well as quantitatively resembles its bare form. The infrared behavior of the result satisfies the constraints imposed by gauge invariance, i.e. the Slavnov-Taylor identities: For vanishing incoming or outgoing ghost momentum, the vertex remains bare. In the generally unknown infrared limit of the gluon momentum, the vertex also remains approximately bare, confirming Zwanziger's hypothesis. On account of asymptotic freedom, the tree-level value is attained in the ultraviolet. Very similar results have been obtained using another vertex input motivated by the Slavnov-Taylor identity. The mapping of the iteration has shown to be quite insensitive to the starting point and always yields an output close to the bare vertex.

The non-perturbative propagators which were employed from previous studies had been calculated with a bare ghost-gluon vertex as an ansatz. The outcome of the calculations in this thesis justify this assumption a posteriori and provide a more profound confirmation of the features of the propagators, in particular gluon confinement in the four-dimensional vacuum theory. For the three-dimensional investigations, support is given for remnant long-range interactions in the high-temperature phase of Yang-Mills theory.

Having verified Zwanziger's hypothesis, the evidence is strengthened for the Zwanziger-Gribov confinement scenario and the associated understanding that the Green functions

of Yang-Mills theory are dominated by ghosts in the infrared. Gluon confinement is thus understood to be due to long-range correlations mediated by ghost interactions. While this is a property of the propagators, the ghost-gluon vertex itself has also shown to be dominated by ghosts in the infrared and by gluons in the intermediate momentum regime.

The error of the results is determined by the truncation adopted for solving the Dyson-Schwinger equation. Due to the mutual coupling of the Green functions, the error of the ghost-gluon vertex is influenced by the one of the propagators. These were analytically solved in the infrared and in the ultraviolet. The vertex is therefore likely to be trustworthy in these momentum regimes as well. Furthermore, the Slavnov-Taylor identity proved certain infrared limits to be correct and perturbation theory ensures the validity of the results in the ultraviolet. Hence, the error for intermediate momenta is the only one which has to be vaguely estimated. A helpful piece of information here are results from lattice calculations which showed a good agreement with the results found here.

Future studies of Yang-Mills theory in Landau gauge are now provided with a consolidated argument for choosing a bare ghost-gluon vertex as an approximation. A less divergent gauge than others, the Landau gauge has proven to be well-suited for an intensified focus on Dyson-Schwinger investigations of Yang-Mills theory and also the theory of Quantum Chromodynamics.

Part of the results obtained here is to be published:

- W. S., A. Maas, J. Wambach, R. Alkofer, *The ghost-gluon vertex in Landau gauge Yang-Mills theory*, <http://arxiv.org/abs/hep-ph/0411060>, to be published in the proceedings of the "International School of Subnuclear Physics 2004", Erice, Italy
- W. S., A. Maas, J. Wambach, R. Alkofer, *Infrared behaviour of the ghost-gluon vertex in Landau gauge Yang-Mills theory*, <http://arxiv.org/abs/hep-ph/0411052>, submitted to Phys. Lett. B

Acknowledgments

First of all, I would like to thank Jochen Wambach for giving me the opportunity to write this thesis and for supporting collaborations. In particular, I am thankful to him for allowing me to participate in the International School of Subnuclear Physics in Erice, Italy.

Especially, I am deeply grateful to Axel Maas for supervising me throughout this work with lots of patience and unconditional backup.

My gratitude goes to Reinhard Alkofer for inspiring most of the topics of this thesis and always having helpful advice.

I am grateful to many people I had valuable discussions with, especially Christian S. Fischer, Dominik Nickel, Peter Watson, Burghard Grüter and Jan M. Pawłowski.

I am indebted to the NHQ group for giving me all kinds of support.

My special gratefulness goes to my family and friends for always being there for me.

Last not least, I want to express my gratitude to my fiancée Colleen for her understanding and encouragement.

A Notations

A.1 Conventions

- The metric $g_{\mu\nu}$ defined by $p \cdot x = g_{\mu\nu} p^\mu x^\nu$ is Euclidian in all calculations:

$$g_{\mu\nu} = \delta_{\mu\nu}$$

A distinction between covariant and contravariant tensorial structures is therefore not necessary.

- Natural units are used where

$$\hbar = c = 1 .$$

In this system we have

$$[\text{length}] = [\text{time}] = [\text{energy}]^{-1} = [\text{mass}]^{-1} .$$

- Greek as well as Latin indices are summed.
- For momentum integrals the shorthand

$$\bar{d}^d p := \frac{d^d p}{(2\pi)^d}$$

is used.

- Integral measures are abbreviated in an intuitive manner,

$$d[xyz] = dx dy dz , \quad \mathcal{D}[A\bar{c}c] = \mathcal{D}A \mathcal{D}\bar{c} \mathcal{D}c . \quad (69)$$

A.2 Structure constants

The contractions of structure constants that occur in the loop graphs of both the DSE for the propagators and the DSE for the ghost-gluon vertex can be computed using the algebra of the Lie group

$$[X^a, X^b] = i f^{abc} X^c , \quad (70)$$

where the X^a are the generators of the group. One can now define the adjoint representation by the matrices

$$[T^a]^{bc} \equiv -i f^{abc} \quad (71)$$

that suffice the same algebra. For $SU(N_c)$, the contractions yield

$$f^{acd} f^{bcd} = N_c \delta^{ab} \quad (72)$$

$$f^{ade} f^{beg} f^{cgd} = \frac{1}{2} N_c f^{abc} \quad (73)$$

B Derivation of the DSE for the ghost-gluon vertex

To derive the DSE for the ghost-gluon vertex it is only necessary to consider an action that involves all contributions from ghosts, although due to the mutual coupling of the Green functions, the entire Lagrangian is implicitly relevant. The ghost part of the action of Yang-Mills theories reads

$$\mathcal{S}_{gh}[A, c, \bar{c}] = \int d^d x (\bar{c}^a \partial^2 c^a + g_d f^{abc} \bar{c}^a \partial_\mu A_\mu^c c^b) . \quad (74)$$

We introduce J_μ^a , $\bar{\sigma}^a$ and σ^a as sources for the fields A_μ^a , c^a and \bar{c}^a , respectively, so that we can define the generating functionals Z , W and Γ according to (20), (4) and (10). The fields and sources are then given by

$$\begin{aligned} \frac{\delta W}{\delta \sigma^a} &= \bar{c}^a, & \frac{\delta W}{\delta \bar{\sigma}^a} &= c^a, & \frac{\delta W}{\delta J_\mu^a} &= A_\mu^a, \\ \frac{\delta \Gamma}{\delta c^a} &= \bar{\sigma}^a, & \frac{\delta \Gamma}{\delta \bar{c}^a} &= \bar{\sigma}^a, & \frac{\delta \Gamma}{\delta A_\mu^a} &= J_\mu^a, \end{aligned} \quad (75)$$

where we use left and right derivatives for Grassmann fields as described in section 3.

Following the steps from eq. (30), one possible way of writing down a DSE is to start with

$$\begin{aligned} 0 &= \int \mathcal{D}[A\bar{c}c] \frac{\delta}{\delta \bar{c}^b(y)} \exp \left\{ -\mathcal{S}_{gh}[A, c, \bar{c}] + \int d^d x (A_\mu^a J_\mu^a + \bar{\sigma}^a c^a + \bar{c}^a \sigma^a) \right\} \\ &= \left\langle -\frac{\delta \mathcal{S}_{gh}[A, c, \bar{c}]}{\delta \bar{c}^b(y)} + \sigma^b(y) \right\rangle . \end{aligned} \quad (76)$$

Retaining non-zero sources we now apply the variation

$$\frac{\delta}{\delta c^c(z)} = \int d^d v \frac{\delta^2 \Gamma}{\delta \bar{c}^d(v) \delta c^c(z)} \frac{\delta}{\delta \sigma^d(v)} + \text{vanishing terms} . \quad (77)$$

Some terms vanish because the functionals can depend only on pairs of Grassmann fields. Throughout the calculation, great care is mandatory when dropping terms since most of them vanish only when setting sources to zero. However, for the sake of readability, vanishing terms are discarded beforehand.

Equation (76) then yields

$$0 = \int d^d v \frac{\delta^2 \Gamma}{\delta \bar{c}^d(v) \delta c^c(z)} \left\langle \frac{\delta \mathcal{S}_{gh}}{\delta \bar{c}^b(y)} \bar{c}^d(v) - \delta^{bd} \delta(y-v) - \sigma^b(y) \bar{c}^d(v) \right\rangle . \quad (78)$$

The last term in the above equation will not contribute. To deal with the first term in eq. (78) we use

$$\frac{\delta \mathcal{S}_{gh}}{\delta \bar{c}^b(y)} = \partial^y c^b(y) + g_d f^{bgh} \partial_\rho^y A_\rho^h(y) c^g(y) . \quad (79)$$

B DERIVATION OF THE DSE FOR THE GHOST-GLUON VERTEX

Omitting source terms, the emerging full 2-point correlation function can be rewritten using $\langle c^a(y)\bar{c}^d(v) \rangle = \frac{\delta^2 W}{\delta \bar{\sigma}^a(y)\delta \sigma^d(v)}$ as shown in (7) and after usage of the relation

$$\delta(x-y)\delta^{ab} = \frac{\delta \bar{\sigma}^b(y)}{\delta \bar{\sigma}^a(x)} = \int d^d z \frac{\delta \bar{\sigma}^b(y)}{\delta \bar{c}^d(z)} \frac{\delta \bar{c}^d(z)}{\delta \bar{\sigma}^a(x)} = \int d^d z \frac{\delta^2 \Gamma}{\delta \bar{c}^d(z)\delta c^b(y)} \frac{\delta^2 W}{\delta \bar{\sigma}^a(x)\delta \sigma^d(z)} \quad (80)$$

equation (78) turns into

$$\begin{aligned} \frac{\delta^2 \Gamma}{\delta \bar{c}^b(y)\delta c^c(z)} Z[J, \bar{\sigma}, \sigma] &= \partial^2 \delta^{bc} \delta(y-z) Z[J, \bar{\sigma}, \sigma] \\ &+ g_a f^{bgh} \partial_\rho^y \int d^d v \frac{\delta^2 \Gamma}{\delta \bar{c}^d(v)\delta c^c(z)} \langle A_\rho^h(y) c^g(y) \bar{c}^d(v) \rangle . \end{aligned} \quad (81)$$

Form here, setting sources to zero directly leads to the DSE for the ghost propagator. To see this, we have to decompose the full 3-point correlation function making use of the identity (8) and then set all sources to zero (abbreviated by $\eta \equiv 0$) to find

$$\begin{aligned} \langle A_\mu^a(x) c^b(y) \bar{c}^c(z) \rangle &= \frac{\delta^3 W}{\delta J_\mu^a(x) \delta \bar{\sigma}^b(y) \delta \sigma^c(z)} \\ &= \frac{\delta}{\delta J_\mu^a(x)} \int d^d [st] \frac{\delta^2 W}{\delta \bar{\sigma}^b(y) \delta \sigma^m(s)} \frac{\delta^2 \Gamma}{\delta \bar{c}^m(s) \delta c^n(t)} \frac{\delta^2 W}{\delta \bar{\sigma}^n(t) \delta \sigma^c(z)} \\ &= \int d^d [rst] \frac{\delta^2 W}{\delta J_\mu^a(x) \delta J_\lambda^k(r)} \frac{\delta^2 W}{\delta \bar{\sigma}^b(y) \delta \sigma^m(s)} \frac{\delta^3 \Gamma}{\delta A_\lambda^k(r) \delta \bar{c}^m(s) \delta c^n(t)} \frac{\delta^2 W}{\delta \bar{\sigma}^n(t) \delta \sigma^c(z)} \\ &\quad + 2 \cdot \frac{\delta^3 W}{\delta J_\mu^a(x) \delta \bar{\sigma}^b(y) \delta \sigma^c(z)} \\ &\stackrel{\eta \equiv 0}{=} - \int d^d [rst] \tilde{D}_{\mu\lambda}^{ak}(x-r) \tilde{D}_G^{bm}(y-s) \tilde{\Gamma}_\lambda^{kmn}(r; s, t) \tilde{D}_G^{nc}(t-z) , \end{aligned} \quad (82)$$

defining the ghost and gluon propagators in position space

$$\tilde{D}_G^{ab}(x-y) := \left. \frac{\delta^2 W}{\delta \bar{c}^a(x) \delta c^b(y)} \right|_{\eta \equiv 0} , \quad (83)$$

$$\tilde{D}_{\mu\nu}^{ab}(x-y) := \left. \frac{\delta^2 W}{\delta J_\mu^a(x) \delta J_\nu^b(y)} \right|_{\eta \equiv 0} , \quad (84)$$

as well as the proper ghost-gluon vertex in position space

$$\tilde{\Gamma}_\mu^{abc}(x; y, z) := \left. \frac{\delta^3 \Gamma}{\delta A_\mu^a(x) \delta \bar{c}^b(y) \delta c^c(z)} \right|_{\eta \equiv 0} . \quad (85)$$

B DERIVATION OF THE DSE FOR THE GHOST-GLUON VERTEX

Plugging this into eq. (81) directly yields the DSE for the ghost propagator in position space. To find the DSE for the ghost-gluon vertex, we maintain the sources at non-zero values and apply to equation (81) the derivative

$$\frac{\delta}{\delta A_\mu^a(x)} = \int d^d u \frac{\delta^2 \Gamma}{\delta A_\mu^a(x) \delta A_\nu^e(u)} \frac{\delta}{\delta J_\nu^e(u)} + \text{vanishing terms} . \quad (86)$$

Since all the necessary derivatives are performed after this, one can immediately set sources to zero to find the proper ghost-gluon vertex:

$$\begin{aligned} \tilde{\Gamma}_\mu^{abc}(x; y, z) &= g_d f^{bgh} \partial_\rho^y \int d^d v \frac{\delta^3 \Gamma}{\delta A_\mu^a(x) \delta \bar{c}^d(v) \delta c^c(z)} \langle A_\rho^h(y) c^g(y) \bar{c}^d(v) \rangle \Big|_{\eta=0} \\ &+ g_d f^{bgh} \partial_\rho^y \int d^d [uv] \frac{\delta^2 \Gamma}{\delta \bar{c}^d(v) \delta c^c(z)} \frac{\delta^2 \Gamma}{\delta A_\mu^a(x) \delta A_\nu^e(u)} \langle A_\rho^h(y) A_\nu^e(u) c^g(y) \bar{c}^d(v) \rangle \Big|_{\eta=0} \end{aligned} \quad (87)$$

According to (9), the decomposition of the full 4-point correlation function using (82) yields

$$\begin{aligned} &\langle A_\rho^h(y) A_\nu^e(u) c^g(y) \bar{c}^d(v) \rangle \Big|_{\eta=0} \\ &= \frac{\delta^2 W}{\delta J_\rho^h(y) \delta J_\nu^e(u)} \frac{\delta^2 W}{\delta \bar{\sigma}^g(y) \delta \sigma^d(v)} \Big|_{\eta=0} + \frac{\delta}{\delta J_\rho^h(y)} \frac{\delta^3 W}{\delta J_\nu^e(u) \delta \bar{\sigma}^g(y) \delta \sigma^d(v)} \Big|_{\eta=0} \\ &= \frac{\delta^2 W}{\delta J_\rho^h(y) \delta J_\nu^e(u)} \frac{\delta^2 W}{\delta \bar{\sigma}^g(y) \delta \sigma^d(v)} \Big|_{\eta=0} + \int d^d [rst] \times \\ &\left\{ \frac{\delta^2 W}{\delta J_\nu^e(u) \delta J_\lambda^k(r)} \frac{\delta^2 W}{\delta \bar{\sigma}^g(y) \delta \sigma^m(s)} \frac{\delta^3 \Gamma}{\delta A_\lambda^k(r) \delta \bar{c}^m(s) \delta c^n(t)} \frac{\delta^3 W}{\delta J_\rho^h(y) \delta \bar{\sigma}^n(t) \delta \sigma^d(v)} \right. \\ &\quad - \frac{\delta^3 W}{\delta J_\rho^h(y) \delta J_\nu^e(u) \delta J_\lambda^k(r)} \frac{\delta^2 W}{\delta \bar{\sigma}^g(y) \delta \sigma^m(s)} \frac{\delta^3 \Gamma}{\delta A_\lambda^k(r) \delta \bar{c}^m(s) \delta c^n(t)} \frac{\delta^2 W}{\delta \bar{\sigma}^n(t) \delta \sigma^d(v)} \\ &\quad - \int d^d w \frac{\delta^2 W}{\delta J_\nu^e(u) \delta J_\lambda^k(r)} \frac{\delta^2 W}{\delta J_\rho^h(y) \delta J_\sigma^l(w)} \frac{\delta^2 W}{\delta \bar{\sigma}^g(y) \delta \sigma^m(s)} \\ &\quad \quad \times \frac{\delta^4 \Gamma}{\delta A_\sigma^l(w) \delta A_\lambda^k(r) \delta \bar{c}^m(s) \delta c^n(t)} \frac{\delta^2 W}{\delta \bar{\sigma}^n(t) \delta \sigma^d(v)} \\ &\quad \left. - \frac{\delta^2 W}{\delta J_\nu^e(u) \delta J_\lambda^k(r)} \frac{\delta^3 W}{\delta J_\rho^h(y) \delta \bar{\sigma}^g(y) \delta \sigma^m(s)} \frac{\delta^3 \Gamma}{\delta A_\lambda^k(r) \delta \bar{c}^m(s) \delta c^n(t)} \frac{\delta^2 W}{\delta \bar{\sigma}^n(t) \delta \sigma^d(v)} \right\} \Big|_{\eta=0} . \quad (88) \end{aligned}$$

The last term of the last line in eq. (88) produces a 3PI-graph which, however, cancels in eq. (87) with the first term. We now introduce two further definitions. The proper three-gluon vertex shall be denoted by

$$\tilde{\Gamma}_{\mu\nu\lambda}^{and}(x, w, r) := \frac{\delta^3 \Gamma}{\delta J_\mu^a(x) \delta J_\nu^n(w) \delta J_\lambda^d(r)} \Big|_{\eta=0} , \quad (89)$$

and the proper 4-point Green function involving two gluons and two ghosts is defined by

$$\tilde{\Gamma}_{\sigma\mu}^{nagc}(w, x; t, z) := \frac{\delta^4\Gamma}{\delta A_\sigma^n(w)\delta A_\mu^a(x)\delta\bar{c}^g(t)\delta c^c(z)}\Bigg|_{\eta=0}. \quad (90)$$

After further decompositions of connected into proper 3-point correlation functions equivalent to (82), and using (80), eq. (87) can be rewritten¹⁷ as

$$\begin{aligned} \tilde{\Gamma}_\mu^{abc}(x; y, z) &= g_d f^{abc} \partial_\mu^y \delta(y-x) \delta(y-z) \\ &+ g_d f^{hbm} \partial_\rho^y \int d^d[rstw] \tilde{D}_{\rho\sigma}^{hg}(y-t) \tilde{D}_G^{mn}(y-w) \tilde{\Gamma}_\mu^{and}(x; w, r) \tilde{D}_G^{de}(r-s) \tilde{\Gamma}_\sigma^{g ec}(t; s, z) \\ &+ g_d f^{mbh} \partial_\rho^y \int d^d[rstw] \tilde{D}_G^{hg}(y-t) \tilde{D}_{\rho\nu}^{mn}(y-w) \tilde{\Gamma}_{\mu\nu\lambda}^{and}(x, w, r) \tilde{D}_{\lambda\sigma}^{de}(r-s) \tilde{\Gamma}_\sigma^{egc}(s; t, z) \\ &- g_d f^{mbh} \partial_\rho^y \int d^d[tw] \tilde{D}_G^{hg}(y-t) \tilde{\Gamma}_{\sigma\mu}^{nagc}(w, x; t, z) \tilde{D}_{\rho\sigma}^{mn}(y-w). \end{aligned} \quad (91)$$

The last step to take is to identify the bare ghost-gluon vertex which is derived from the action (74) as

$$\tilde{\Gamma}_\mu^{(0)abc}(x; y, z) := \frac{\delta^3 \mathcal{S}_{gh}}{\delta A_\mu^a(x) \delta \bar{c}^b(y) \delta c^c(z)} = g_d f^{abc} \partial_\mu^y \delta(y-x) \delta(y-z), \quad (92)$$

whence one readily obtains

$$g_d f^{hbm} \partial_\rho^y \tilde{D}_{\rho\sigma}^{hg}(y-t) \tilde{D}_G^{mn}(y-w) = \int d^d[uv] \tilde{\Gamma}_\rho^{(0)hbm}(u; y, v) \tilde{D}_{\rho\sigma}^{hg}(u-t) \tilde{D}_G^{mn}(v-w). \quad (93)$$

Using this relation, one can remove the spacetime derivatives in favor of bare ghost-gluon vertices and finally arrive at the complete DSE for the ghost-gluon vertex in position space:

$$\begin{aligned} \tilde{\Gamma}_\mu^{abc}(x; y, z) &= \tilde{\Gamma}_\mu^{(0)abc}(x; y, z) \\ &+ \int d^d[rstuvw] \tilde{D}_G^{mn}(v-w) \tilde{\Gamma}_\mu^{and}(x; w, r) \tilde{D}_G^{de}(r-s) \tilde{\Gamma}_\sigma^{g ec}(t; s, z) \tilde{D}_{\rho\sigma}^{hg}(u-t) \tilde{\Gamma}_\mu^{(0)hbm}(u; y, v) \\ &+ \int d^d[rstuvw] \tilde{D}_{\rho\nu}^{mn}(u-w) \tilde{\Gamma}_{\mu\nu\lambda}^{and}(x, w, r) \tilde{D}_{\lambda\sigma}^{de}(r-s) \tilde{\Gamma}_\sigma^{egc}(s; t, z) \tilde{D}_G^{hg}(v-t) \tilde{\Gamma}_\rho^{(0)mbh}(u; y, v) \\ &- \int d^d[tuvw] \tilde{D}_G^{gh}(v-t) \tilde{\Gamma}_{\sigma\mu}^{nagc}(w, x; t, z) \tilde{D}_{\rho\sigma}^{mn}(u-w) \tilde{\Gamma}_\mu^{(0)mbh}(u; y, v) \end{aligned} \quad (94)$$

Applying a Fourier transform with one incoming and one outgoing ghost momentum¹⁸ such as

$$\Gamma_\mu^{(0)abc}(k; q, p) = \int d^d[xyz] \tilde{\Gamma}_\mu^{(0)abc}(x; y, z) e^{i(k \cdot x - q \cdot y + p \cdot z)} = i g_d q_\mu f^{abc} = g_d f^{abc} \Gamma_\mu^{(0)}(q) \quad (95)$$

¹⁷The indices and integration variables have been renamed in a convenient way.

¹⁸Here, the incoming antighost is conjugated into a ghost with reversed momentum.

defines the bare ghost-gluon vertex in momentum space. Following this convention, all Green functions in momentum space (symbols with tilde) may be Fourier transformed into momentum space (symbols without tilde), and one obtains the DSE for the ghost-gluon vertex as it is shown in fig. 13 and written down explicitly, although excluding the four-point function, in momentum space in eq. (36).

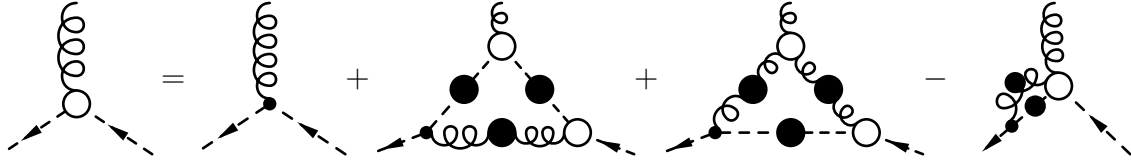


Figure 13: Complete DSE for the ghost-gluon vertex

C Integrals

C.1 Vector integrals

The vector integrals one has to deal with when performing vertex calculations with three external legs have either one or two scales. A vector integral with one scale is of the form

$$I_\mu(q) = \int \bar{d}^d \omega \omega_\mu f(\omega \cdot q, \omega^2, q^2, k^2) = q_\mu I(q^2), \quad (96)$$

with some arbitrary function f that depends on the angle between q and the integration variable ω and may depend on any other scale as long as there is no angle with ω involved. Due to Lorentz invariance, $I_\mu(q)$ must be proportional to q_μ , the proportionality factor can be found by contracting (96) on both sides with q_μ :

$$I(q^2) = \frac{1}{q^2} q_\mu I_\mu(q) \quad (97)$$

A vector integral with two external scales generally looks like

$$I_\mu(q, k) = \int \bar{d}^d \omega \omega_\mu f(\omega \cdot q, \omega \cdot k, \omega^2, q^2, k^2) = q_\mu I_q(q^2) + k_\mu I_k(k^2). \quad (98)$$

The scalar integrals $I_q(q^2)$ and $I_k(k^2)$ are found by contracting (98) once with q_μ and once with k_μ

$$I_q(q^2) = \frac{1}{\Delta} (k^2 q_\mu I_\mu(q, k) - q \cdot k k_\mu I_\mu(q, k)) \quad (99)$$

$$I_k(k^2) = \frac{1}{\Delta} (q^2 k_\mu I_\mu(q, k) - q \cdot k q_\mu I_\mu(q, k)) \quad (100)$$

where $\Delta = q^2 k^2 - (q \cdot k)^2$ is the so-called Gram determinant.

C.2 Tensor integrals

One also encounters integrals of the form

$$I_{\mu\nu}(k) = \int \bar{d}^d \omega \omega_\mu \omega_\nu f(\omega \cdot k, \omega^2). \quad (101)$$

Since this object has two Lorentz indices and one scale k one can write

$$I_{\mu\nu}(k) = k_\mu k_\nu I_1(k^2) + \delta_{\mu\nu} k^2 I_2(k^2), \quad (102)$$

$k_\mu k_\nu$ and $\delta_{\mu\nu}$ being the only Lorentz invariants with two indices. By contraction with the transverse projector and with the metric one finds

$$I_2(k^2) = \frac{1}{(d-1)k^2} t_{\mu\nu}(k) I_{\mu\nu}(k), \quad (103)$$

$$I_1(k^2) = \frac{1}{k^2} \delta_{\mu\nu} I_{\mu\nu}(k) - d I_2(k^2). \quad (104)$$

C.3 Two-point integral

The two-point integrals,

$$\Xi^{(d)}(\alpha, \beta; q) := \int \frac{\bar{d}^d \omega}{(\omega^2)^\alpha ((\omega - q)^2)^\beta}, \quad (105)$$

which are encountered in the calculations can be shown to be homogeneous functions of the momentum q . By a scaling of the integration variable, $\omega \rightarrow \lambda\omega$, one readily obtains

$$\Xi^{(d)}(\alpha, \beta; \lambda q) = \lambda^{d-2\alpha-2\beta} \Xi^{(d)}(\alpha, \beta; q). \quad (106)$$

For the two-point integral can only depend on the scale, it must be of the form $\Xi^{(d)}(\alpha, \beta; q) \sim q^\kappa$. The exponent of the power law can be determined by eq. (106) to find $\kappa = d - 2\alpha - 2\beta$.

Two-point integrals can be calculated explicitly using Feynman parameters such as in

$$\frac{1}{C_1^\alpha C_2^\beta} = \int_0^1 dx \frac{x^{\alpha-1} (1-x)^{\beta-1}}{(xC_1 + (1-x)C_2)^{\alpha+\beta}} \frac{1}{B(\alpha, \beta)}, \quad (107)$$

where $B(\alpha, \beta)$ is the Euler beta function, and

$$\int \frac{\bar{d}^d \ell}{(\ell^2 + \Delta)^n} = \frac{1}{(4\pi)^{d/2}} \frac{\Gamma(n - d/2)}{\Gamma(n)} \left(\frac{1}{\Delta}\right)^{n-d/2}. \quad (108)$$

Applying this trick to the integrand in (105) one obtains

$$\begin{aligned}
 \Xi^{(d)}(\alpha, \beta; q) &= \int_0^1 dx \int \frac{\bar{d}^d \omega x^{\alpha-1} (1-x)^{\beta-1}}{(\omega^2(1-x) + x(\omega-q)^2)^{\alpha+\beta}} \frac{1}{B(\alpha, \beta)} \\
 &= \frac{1}{B(\alpha, \beta)} \int_0^1 dx x^{\alpha-1} (1-x)^{\beta-1} \int \frac{\bar{d}^d \ell}{(\ell^2 + \Lambda)^{\alpha+\beta}} \\
 &= \frac{1}{B(\alpha, \beta)} \frac{1}{(4\pi)^{d/2}} \frac{\Gamma(\alpha + \beta - d/2)}{\Gamma(\alpha + \beta)} \int_0^1 dx x^{\alpha-1} (1-x)^{\beta-1} \Lambda^{d/2-\alpha-\beta} \\
 &= \frac{1}{(4\pi)^{d/2}} \frac{\Gamma(\alpha + \beta - d/2)}{\Gamma(\alpha)\Gamma(\beta)} \frac{\Gamma(d/2 - \alpha)\Gamma(d/2 - \beta)}{\Gamma(d - \alpha - \beta)} (q^2)^{d/2-\alpha-\beta} \quad (109)
 \end{aligned}$$

where we have assigned $\ell \equiv \omega - xq$ and $\Lambda \equiv q^2 x(1-x)$. Note that the power law behavior follows the prediction from above. For the special case $d = 4$ and $\alpha = \beta = 1$ the two-point integral (109) with the expansion of the gamma function $\Gamma(\epsilon) = 1/\epsilon + \mathcal{O}(1)$ yields a simple $1/\epsilon$ -pole. For $d = 3$ and $\alpha = \beta = 1$ we are taken to the result (60).

C.4 Triangle integral

For the triangle integral over d -dimensional Euclidian spacetime,

$$\Phi^{(d)}(\alpha, \beta, \gamma; k, q, p) := \int \frac{\bar{d}^d \omega}{(\omega^2)^\alpha ((\omega - q)^2)^\beta ((\omega + k)^2)^\gamma}, \quad (110)$$

a solution with general values for the exponents α, β, γ is not known. The usual trick introducing Feynman parameters leads to analytically insolvable parameter integrals. Here, another method is used to end up at a new integral representation which might lead to analytical solutions of specific cases.

The denominators in (110) can be rewritten in terms of gamma functions,

$$\frac{1}{A^\alpha} = \frac{1}{\Gamma(\alpha)} \int_0^\infty dx x^{\alpha-1} e^{-Ax}, \quad (111)$$

leading to a Gaussian integral of ω that can be performed to yield after some algebra

$$\Phi^{(d)}(\alpha, \beta, \gamma; k, q, p) = \frac{\Gamma(\alpha + \beta + \gamma - d/2)}{(4\pi)^{d/2} \Gamma(\alpha)\Gamma(\beta)\Gamma(\gamma)} \int_0^1 d[xyz] \frac{x^{\alpha-1} y^{\beta-1} z^{\gamma-1}}{(xyk^2 + xzq^2 + yzp^2)^{\alpha+\beta+\gamma-d/2}} \quad (112)$$

For a ‘‘unique’’ triangle, defined by $\alpha + \beta + \gamma = d$, a compact result can be obtained (cf. [Vas81]),

$$\Phi^{(d)}(\alpha, \beta, \gamma; k, q, p) \Big|_{\alpha+\beta+\gamma=d} = \frac{\Gamma(\alpha + \beta + \gamma - d/2)}{(4\pi)^{d/2} \Gamma(\alpha)\Gamma(\beta)\Gamma(\gamma)} \frac{1}{(k^2)^{d/2-\alpha} (q^2)^{d/2-\beta} (p^2)^{d/2-\gamma}}. \quad (113)$$

The integral $\Phi^{(3)}(1, 1, 1; k, q, p)$ therefore yields the result (59), in agreement with [Pel71]. There also exist a way to calculate this specific integral using conformal inversion $\vec{\omega} \rightarrow \vec{\omega}/\omega^2$ [Arn97].

For a numerical solution of the triangle integral it is advisory to take the pole structure of the integrand into account. The Gauss-Legendre points which were used for the calculations in section 6.2 were laid carefully around the poles. Parametrising the integral (110) by spherical coordinates, q, k and $q \cdot k =: qk \cos \gamma$, one can define the azimuthal angle $\theta_{(d-1)}$ by $\omega \cdot q = \omega q \cos \theta_{(d-1)}$ and the next angle $\theta_{(d-2)}$ by $\omega \cdot k = \omega k (\sin \theta_{(d-1)} \cos \theta_{(d-2)} \sin \gamma + \cos \theta_{(d-1)} \cos \gamma)$. Note that $\theta_1 \in [0, 2\pi)$ whereas $\theta_k \in [0, \pi) \forall \{k, 1 < k \leq d-1\}$. The integrand then becomes singular for $\{\omega = q, \theta_{(d-1)} = 0, \forall \theta_{(d-2)}\}$ and $\{\omega = k, \theta_{(d-1)} = \pi - \gamma, \theta_{(d-2)} = \pi\}$.

D Integral kernels

The integral kernels A_1 through A_6 and B_1 through B_6 in eqs. (38a) and (38b) are given by

$$\begin{aligned}
 A_1 &= (k \cdot w q \cdot k - k^2 q \cdot w)(q^2 w^2 + k \cdot w(q^2 - q \cdot w) + q \cdot k(w^2 - q \cdot w) - \\
 &\quad q^2 q \cdot w - w^2 q \cdot w + (q^2 + w^2 - 2q \cdot w)q \cdot w + (q \cdot w)^2) \\
 A_2 &= 2(w^2(q \cdot k)^3(k^2 + w \cdot k) - w^2(q \cdot k)^2(w^2 - q \cdot w)(k^2 + w \cdot k) + \\
 &\quad (k \cdot w)^2 q \cdot k q \cdot w(k^2 + w \cdot k) + k^2(q^2 w^2 - (q \cdot w)^2)(w^2(k^2 + w \cdot k) + \\
 &\quad q \cdot w(w^2 + w \cdot k)) + k^2 q \cdot k(-q^2 w^2(k^2 + w \cdot k) - (q \cdot w)^2(w^2 + w \cdot k) + \\
 &\quad w^2 q \cdot w(k^2 + w^2 + 2w \cdot k)) + k \cdot w(-(q \cdot k)^2(w^2 + q \cdot w)(k^2 + w \cdot k) + \\
 &\quad q \cdot k(w^2 q \cdot w(k^2 + w \cdot k) + (q \cdot w)^2(w^2 + w \cdot k) - q^2 w^2(k^2 + w^2 + 2w \cdot k)) + \\
 &\quad k^2(-(q \cdot w)^2(k^2 + w \cdot k) - q^2 w^2(w^2 + w \cdot k) + q^2 q \cdot w(k^2 + w^2 + 2w \cdot k))) \\
 A_3 &= (q^2 - q \cdot w)(w^2 + k \cdot w - q \cdot k - q \cdot w)(-(k \cdot w)q \cdot k + k^2 q \cdot w) \\
 A_4 &= q \cdot w(k^2 q \cdot k q \cdot w(w^2 + 2w \cdot k) + w^2(q \cdot k)^2(k^2 + w^2 + 2w \cdot k) - \\
 &\quad (k \cdot w)^2 q \cdot k(2k^2 + w^2 + 2w \cdot k) + k^2(k^2 w^2 q \cdot w + (q \cdot w)^2(w^2 + 2w \cdot k) - q^2 w^2 \\
 &\quad (k^2 + w^2 + 2w \cdot k)) + k \cdot w((q \cdot k)^2(2k^2 + w^2 + 2w \cdot k) - q \cdot k(w^2(k^2 + q \cdot w) + \\
 &\quad 2q \cdot w w \cdot k) + k^2(-2q^2(k^2 + w^2 + 2w \cdot k) + q \cdot w(2k^2 + w^2 + 2w \cdot k))) \\
 A_5 &= (-k^2 + w^2)(w^2 + k \cdot w - q \cdot k - q \cdot w) \times \\
 &\quad (-w^2(q \cdot k)^2 + k \cdot w q \cdot k q \cdot w + k^2(q^2 w^2 - (q \cdot w)^2)) \\
 A_6 &= k^2(w^2 + k \cdot w - q \cdot k - q \cdot w)q \cdot w(k \cdot w q \cdot k - k^2 q \cdot w)
 \end{aligned}$$

$$\begin{aligned}
 B_1 &= -(q^2 k \cdot w - q \cdot k q \cdot w)(w^2(q^2 + q \cdot k) + k \cdot w(q^2 - q \cdot w) - q \cdot w(q \cdot k + q \cdot w)) \\
 B_2 &= -w^2(q \cdot k)^4 + w^2(q \cdot k)^3(w^2 - q \cdot w) + k^2 q^2(q^2 w^2 - (q \cdot w)^2)(k^2 + w^2 + 2w \cdot k) - \\
 &\quad (k \cdot w)^2 q \cdot w((q \cdot k)^2 + q^2(k^2 + 2w \cdot k)) + q \cdot k(-k^2 q^2 w^4 + 2w^2(q \cdot w)^2(k^2 + w \cdot k) + \\
 &\quad 2(q \cdot w)^3(w^2 + w \cdot k) - q^2 w^2 q \cdot w(k^2 + 2w^2 + 4w \cdot k)) + (q \cdot k)^2(-q^2 w^2(w^2 + \\
 &\quad 2w \cdot k) - 2w^2 q \cdot w(k^2 + w^2 + 2w \cdot k) + (q \cdot w)^2(k^2 + 3w^2 + 4w \cdot k)) + k \cdot w((q \cdot k)^2 \\
 &\quad \times q \cdot w(-w^2 + q \cdot w) + (q \cdot k)^3(w^2 + q \cdot w) + q^2(-w^2 q \cdot w(k^2 + 2w \cdot k) + 2q^2 w^2 \times \\
 &\quad (k^2 + w^2 + 2w \cdot k) - (q \cdot w)^2(k^2 + 2w^2 + 2w \cdot k)) + q \cdot k(2(q \cdot w)^2(k^2 + w \cdot k) - \\
 &\quad q^2 q \cdot w(k^2 + 2w^2 + 2w \cdot k) + q^2 w^2(k^2 + 2w^2 + 4w \cdot k))) \\
 B_3 &= (q^2 - q \cdot w)(w^2 + k \cdot w - q \cdot k - q \cdot w)(q^2 k \cdot w - q \cdot k q \cdot w) \\
 B_4 &= q \cdot w(k^2 q^2(-w^2 + q \cdot w)(k^2 + w^2 + 2w \cdot k) - q \cdot k q \cdot w(w^2(k^2 + q \cdot w) + \\
 &\quad 2q \cdot w w \cdot k) + (k \cdot w)^2((q \cdot k)^2 + q^2(k^2 + w^2 + 2w \cdot k)) + (q \cdot k)^2(w^2(k^2 + w^2 + \\
 &\quad 2w \cdot k) - q \cdot w(k^2 + 2w^2 + 4w \cdot k)) + k \cdot w(-(q \cdot k)^3 + (q \cdot k)^2(w^2 - q \cdot w) + \\
 &\quad q^2 q \cdot w(k^2 + w^2 + 2w \cdot k) + q \cdot k(q^2(k^2 + w^2 + 2w \cdot k) - \\
 &\quad q \cdot w(2k^2 + w^2 + 2w \cdot k)))) \\
 B_5 &= -(w^2 + k \cdot w - q \cdot k - q \cdot w)(w^2 q \cdot k(-k^2 q^2 + (q \cdot k)^2) + \\
 &\quad k \cdot w(q^2 w^2 - (q \cdot k)^2) q \cdot w + (k - w)(k + w) q \cdot k (q \cdot w)^2) \\
 B_6 &= q \cdot k q \cdot w(-w^2 - k \cdot w + q \cdot k + q \cdot w)(k \cdot w q \cdot k - k^2 q \cdot w)
 \end{aligned}$$

E Infrared limits

In section 6.2, the infrared limits of any of the momenta of the vertex were studied. If one of the momenta is taken to zero, the other two momenta may remain finite but equal in magnitude, due to momentum conservation. Thus one obtains $A(x^2; 0, x^2)$, $A(x^2; x^2, 0)$ or $A(0; x^2, x^2)$, for example. The limit $\lim_{x \rightarrow 0}$ should then yield the same value for all three of the above cases. But as one can see from the comparison of figures 5, 6 and 7 as well as from figure 9, it does not. So the infrared limits of the results seem to be non-uniform at first glance. The explanation for this effect is found in the notation. The way the infrared limits are obtained is such that the functions are not ever evaluated with one momentum exactly at zero because the kernel would diverge. Instead, this momentum is chosen to be much smaller than x . From investigations shown in figure 14 it is found that at about $x/1000$ the value of the integral approaches a constant and so one can extrapolate to zero retaining the same constant. So $A(x^2; 0, x^2)$ is really supposed to be understood as $A(x^2; 10^{-6}x^2, x^2)$. Therefore it is not surprising that the limit $\lim_{x \rightarrow 0}$ does not yield the same value for either $\lim_{x \rightarrow 0} A(x^2; 0, x^2)$, $\lim_{x \rightarrow 0} A(x^2; x^2, 0)$ or $\lim_{x \rightarrow 0} A(0; x^2, x^2)$ since these are nevertheless different momentum configurations. Mathematically spoken, the infrared limits of the function A (or B , resp.) are not interchangeable. Moreover, any infrared limit of the kind $\lim_{x \rightarrow 0} A(ax^2; bx^2, cx^2)$ depends on the geometry of the triangle spanned by the momenta. On the other hand, the vertex Γ_μ is not as sensitive to these

ambiguities for it multiplies the function A and B with a momentum vector. For all momenta at zero, the vertex therefore vanishes.

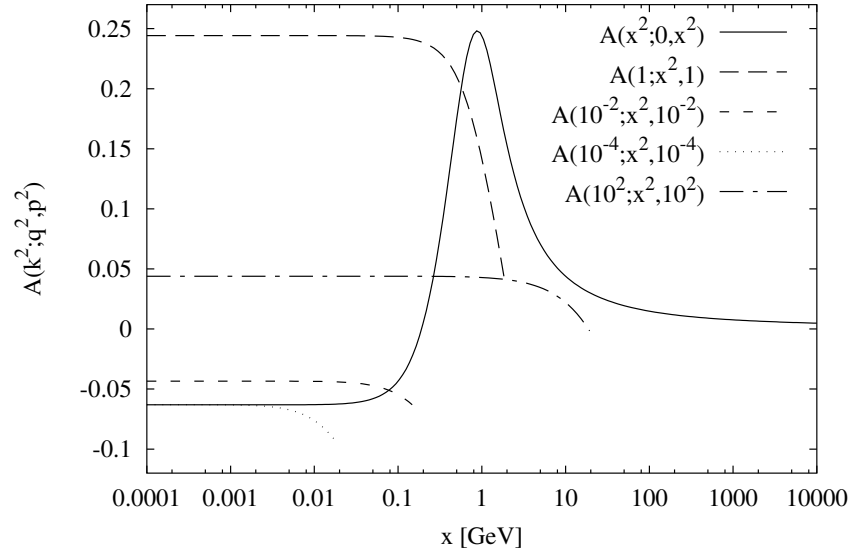


Figure 14: Numerical procedure of taking infrared limits. It is shown that if one momentum is much smaller than the others, the function A approaches a constant.

References

- [Alk01] Alkofer, Reinhard and von Smekal, Lorenz, *The infrared behavior of QCD Green's functions: Confinement, dynamical symmetry breaking, and hadrons as relativistic bound states*, Phys. Rept. **353** (2001), 281.
- [Alk03] Alkofer, Reinhard and Fischer, Christian S. and von Smekal, Lorenz, *Infrared exponents and the running coupling of Landau gauge QCD and their relation to confinement*, Eur. Phys. J. **A17** (2003), 773.
- [Alk04a] Alkofer, R. and Detmold, W. and Fischer, C. S. and Maris, P., *Analytic properties of the Landau gauge gluon and quark propagators*, Phys. Rev. **D70** (2004), 014014.
- [Alk04b] Alkofer, Reinhard, *private communication*.
- [App81] Appelquist, Thomas and Pisarski, Robert D., *High-temperature Yang-Mills theories and three-dimensional quantum chromodynamics*, Phys. Rev. **D23** (1981), 2305.
- [Arn97] Arnold, Peter and Wright, David, *The tricritical point of finite-temperature phase transitions in large N (Higgs) gauge theories*, Phys. Rev. **D55** (1997), 6274–6286.
- [Bal80] Ball, James S. and Chiu, Ting-Wai, *Analytic properties of the vertex function in gauge theories. 1*, Phys. Rev. **D22** (1980), 2542.
- [Bec75] Becchi, C. and Rouet, A. and Stora, R., *Renormalization of the Abelian Higgs-Kibble model*, Commun. Math. Phys. **42** (1975), 127–162.
- [Bjo65] Bjorken, J. D. and Drell, S. D., *Relativistic quantum fields*, New York, USA: McGraw-Hill (1965).
- [Blo03] Bloch, J. C. R., *Two-loop improved truncation of the ghost-gluon Dyson-Schwinger equations: Multiplicatively renormalizable propagators and nonperturbative running coupling*, Few Body Syst. **33** (2003), 111–152.
- [Bou98a] Boucaud, P. and Leroy, J. P. and Micheli, J. and Pene, O. and Roiesnel, C., *Lattice calculation of $\alpha(s)$ in momentum scheme*, JHEP **10** (1998), 017.
- [Bou98b] Boucaud, P. and Leroy, J. P. and Micheli, J. and Pene, O. and Roiesnel, C., *Three-loop beta function and non-perturbative $\alpha(s)$ in asymmetric momentum scheme*, JHEP **12** (1998), 004.
- [Bow04] Bowman, Patrick O. and Heller, Urs M. and Leinweber, Derek B. and Parappilly, Maria B. and Williams, Anthony G., *Unquenched gluon propagator in Landau gauge*, Phys. Rev. **D70** (2004), 034509.

REFERENCES

- [Che81] Chetyrkin, K. G. and Tkachov, F. V., *Integration by parts: the algorithm to calculate beta functions in 4 loops*, Nucl. Phys. **B192** (1981), 159–204.
- [Col84] Collins, John C., *Renormalization. An introduction to renormalization, the renormalization group, and the operator product expansion*, Cambridge, Uk: Univ. Pr. (1984) 380p.
- [Cuc01] Cucchieri, A. and Karsch, F. and Petreczky, P., *Propagators and dimensional reduction of hot $SU(2)$ gauge theory*, Phys. Rev. **D64** (2001), 036001.
- [Cuc03] Cucchieri, Attilio and Mendes, Tereza and Taurines, Andre R., *$SU(2)$ Landau gluon propagator on a 140^{*3} lattice*, Phys. Rev. **D67** (2003), 091502.
- [Cuc04] Cucchieri, A. and Mendes, T. and Mihara, A., *Numerical study of the ghost-gluon vertex in Landau gauge*, hep-lat/0408034.
- [Das97] Das, A., *Finite Temperature Field Theory*, World Scientific, 1997.
- [Dav96] Davydychev, Andrei I. and Osland, P. and Tarasov, O. V., *Three-gluon vertex in arbitrary gauge and dimension*, Phys. Rev. **D54** (1996), 4087–4113.
- [Dir64] Dirac, P.A.M., *Lectures on quantum mechanics*, Academic Press (1964).
- [Dys49] Dyson, F. J., *The S matrix in quantum electrodynamics*, Phys. Rev. **75** (1949), 1736.
- [Fad67] Faddeev, L. D. and Popov, V. N., *Feynman diagrams for the Yang-Mills field*, Phys. Lett. **B25** (1967), 29–30.
- [Fel02] Feldmeier, H., *Informationstheorie und Quantenstatistik*, Lecture notes TU Darmstadt, in German (2002).
- [Feu04] Feuchter, C. and Reinhardt, H., *Quark and gluon confinement in Coulomb gauge*, hep-th/0402106.
- [Fis02] Fischer, C. S. and Alkofer, R., *Infrared exponents and running coupling of $SU(N)$ Yang-Mills theories*, Phys. Lett. **B536** (2002), 177–184.
- [Fis03] Fischer, Christian S. and Alkofer, Reinhard, *Non-perturbative propagators, running coupling and dynamical quark mass of Landau gauge QCD*, Phys. Rev. **D67** (2003), 094020.
- [Gre04] Greensite, Jeff and Olejnik, Stefan and Zwanziger, Daniel, *Center vortices and the Gribov horizon*, hep-lat/0407032.
- [Gri78] Gribov, V. N., *Quantization of non-Abelian gauge theories*, Nucl. Phys. **B139** (1978), 1.

REFERENCES

- [Gro73] Gross, D. J. and Wilczek, Frank, *Ultraviolet behavior of non-abelian gauge theories*, Phys. Rev. Lett. **30** (1973), 1343–1346, Nobel prize 2004.
- [Hen92] Henneaux, M. and Teitelboim, C., *Quantization of gauge systems*, Princeton, USA: Univ. Pr. (1992) 520 p.
- [Hoo72] Hooft, Gerard 't and Veltman, M. J. G., *Regularization and renormalization of gauge fields*, Nucl. Phys. **B44** (1972), 189–213, Nobel prize 1999.
- [Itz80] Itzykson, C. and Zuber, J. B., *Quantum field theory*, New York, USA: McGraw-Hill (1980) 705 p. (International Series In Pure and Applied Physics).
- [Kug79] Kugo, Taichiro and Ojima, Izumi, *Local covariant operator formalism of non-abelian gauge theories and quark confinement problem*, Prog. Theor. Phys. Suppl. **66** (1979), 1.
- [Kug95] Kugo, Taichiro, *The universal renormalization factors $Z(1) / Z(3)$ and color confinement condition in non-Abelian gauge theory*, hep-th/9511033.
- [Lae03] Laermann, Edwin and Philipsen, Owe, *Status of lattice QCD at finite temperature*, Ann. Rev. Nucl. Part. Sci. **53** (2003), 163.
- [Lan02] Langfeld, K. and others, *Vortex induced confinement and the IR properties of Green functions*, hep-th/0209173.
- [Ler02] Lerche, Christoph and Smekal, Lorenz von, *On the infrared exponent for gluon and ghost propagation in Landau gauge QCD*, Phys. Rev. **D65** (2002), 125006.
- [Maa04] Maas, Axel and Wambach, Jochen and Gruter, Burghard and Alkofer, Reinhard, *High-temperature limit of Landau-gauge Yang-Mills theory*, Eur. Phys. J. **C37** (2004), 335–357.
- [Mar78] Marciano, William J. and Pagels, Heinz, *Quantum Chromodynamics*, Phys. Rept. **36** (1978), 137.
- [Mut98] Muta, T., *Foundations Of Quantum Chromodynamics*, World Scientific (1998).
- [Nak90] Nakanishi, N. and Ojima, I., *Covariant operator formalism of gauge theories and quantum gravity*, World Sci. Lect. Notes Phys. **27** (1990), 1–434.
- [Pas79] Passarino, G. and Veltman, M. J. G., *One loop corrections for $e^+ e^-$ annihilation into $\mu^+ \mu^-$ in the Weinberg model*, Nucl. Phys. **B160** (1979), 151.
- [Pel71] Peliti, L., D'Ermao, M. and Parisi, G., Lett. Nuovo Cimento **2** (1971), 878.
- [Pes95] Peskin, M.E. and Schroeder, D.V., *An Introduction To Quantum Field Theory*, Westview (1995).

REFERENCES

- [Pol73] Politzer, H. David, *Reliable perturbative results for strong interactions?*, Phys. Rev. Lett. **30** (1973), 1346–1349, Nobel prize 2004.
- [Pre92] Press, William H., Teukolsky, Saul A., Vetterling, William T., Flannery, Brian P., *Numerical recipes in C*, Cambridge University Press (1992).
- [Riv87] Rivers, R. J., *Path integral methods in quantum field theory*, Cambridge, UK: Univ. Pr. (1987) 339 p. (Cambridge monographs on mathematical physics).
- [Rob94] Roberts, Craig D. and Williams, Anthony G., *Dyson-Schwinger equations and their application to hadronic physics*, Prog. Part. Nucl. Phys. **33** (1994), 477–575.
- [Sch51] Schwinger, J. S., *On the Green's functions of quantized fields. I and II*, Proc. Nat. Acad. Sc. **37** (1951), 452,455.
- [Sla72] Slavnov, A. A., *Ward identities in gauge theories*, Theor. Math. Phys. **10** (1972), 99–107.
- [Sme97] Smekal, Lorenz von and Alkofer, Reinhard and Hauck, Andreas , *The infrared behavior of gluon and ghost propagators in Landau gauge QCD*, Phys. Rev. Lett. **79** (1997), 3591–3594.
- [Sme98a] Smekal, Lorenz von, *Perspectives for Hadronic Physics from Dyson-Schwinger Equations for the Dynamics of Quark and Glue*, Habilitation thesis, Universität Erlangen-Nürnberg (1998).
- [Sme98b] Smekal, Lorenz von and Hauck, Andreas and Alkofer, Reinhard , *A solution to coupled Dyson-Schwinger equations for gluons and ghosts in Landau gauge*, Ann. Phys. **267** (1998), 1.
- [Tay71] Taylor, J. C., *Ward identities and charge renormalization of the Yang-Mills field*, Nucl. Phys. **B33** (1971), 436–444.
- [Tka81] Tkachov, F. V., *A theorem on analytical calculability of four loop renormalization group functions*, Phys. Lett. **B100** (1981), 65–68.
- [Vac95] Vachnadze, L. G. and Kiknadze, N. A. and Khelashvili, A. A., *Singular power law infrared asymptotic behavior of the gluon propagator in the covariant gauge*, Theor. Math. Phys. **102** (1995), 34–39.
- [Vas81] Vasiliev, A. N. and Pismak, Yu. M. and Khonkonen, Yu. R., *1/N expansion: calculation of the exponents eta and nu in the order 1/N**2 for arbitrary number of dimensions*, Theor. Math. Phys. **47** (1981), 465–475.
- [Vel94] Veltman, M. J. G., *Diagrammatica: The Path to Feynman rules*, Cambridge, UK: Univ. Pr. (1994) 284 p. (Cambridge lecture notes in physics, 4).

- [Ver00] Vermaseren, J.A.M., *New features of FORM*, [http://www.nikhef.nl/~ form/](http://www.nikhef.nl/~form/) (2000).
- [Wat99] Watson, P., *Perturbative constraints on the Slavnov-Taylor identity for the ghost-gluon vertex in QCD*, hep-ph/9901454.
- [Wat00] Watson, Peter, *The Inclusion of Ghosts in Landau Gauge Schwinger-Dyson Studies of Infrared QCD*, Ph.D. thesis, Physics Department, University Of Durham, England, 2000.
- [Yan54] Yang, Chen-Ning and Mills, R. L., *Conservation of isotopic spin and isotopic gauge invariance*, Phys. Rev. **96** (1954), 191–195.
- [Zwa94] Daniel Zwanziger, *Fundamental modular region, Boltzmann factor and area law in lattice gauge theory*, Nucl. Phys. **B412** (1994), 657–730.
- [Zwa04] Zwanziger, Daniel, *Non-perturbative Faddeev-Popov formula and infrared limit of QCD*, Phys. Rev. **D69** (2004), 016002.